ornl

NUREG/CR-3886
ORNL/TM-9265

OAK RIDGE
NATIONAL
LABORATORY

MARTIN MARIETTA

Activity and Fluence Calculations for the Startup and Two-Year Irradiation Experiments Performed at the Poolside Facility

R. E. Maerker
B. A. Worley

This Work Performed for
U.S. Nuclear Regulatory Commission
Office of Nuclear Regulatory Research
Under Interagency Agreement DOE 40-551-75 and 40-552-75

OPERATED BY
MARTIN MARIETTA ENERGY SYSTEMS, INC.
FOR THE UNITED STATES
DEPARTMENT OF ENERGY

NOTICE

Availability of Reference Materials Cited in NRC Publications

Most documents cited in NRC publications will be available from one of the following sources:

1. The NRC Public Document Room, 1717 H Street, N.W., Washington, DC 20555
2. The NRC/GPO Sales Program, U.S. Nuclear Regulatory Commission, Washington, DC 20555
3. The National Technical Information Service, Springfield, VA 22161

Although the listing that follows represents the majority of documents cited in NRC publications, it is not intended to be exhaustive.

Referenced documents available for inspection and copying for a fee from the NRC Public Document Room include NRC correspondence and internal NRC memoranda; NRC Office of Inspection and Enforcement bulletins, circulars, information notices, inspection and investigation notices; Licensee Event Reports; vendor reports and correspondence; Commission papers; and applicant and licensee documents and correspondence.

The following documents in the NUREG series are available for purchase from the NRC/GPO Sales Program: formal NRC staff and contractor reports, NRC-sponsored conference proceedings, and NRC booklets and brochures. Also available are Regulatory Guides, NRC regulations in the *Code of Federal Regulations*, and *Nuclear Regulatory Commission Issuances*.

Documents available from the National Technical Information Service include NUREG series reports and technical reports prepared by other federal agencies and reports prepared by the Atomic Energy Commission, forerunner agency to the Nuclear Regulatory Commission.

Documents available from public and special technical libraries include all open literature items, such as books, journal and periodical articles, and transactions. *Federal Register* notices, federal and state legislation, and congressional reports can usually be obtained from these libraries.

Documents such as theses, dissertations, foreign reports and translations, and non-NRC conference proceedings are available for purchase from the organization sponsoring the publication cited.

Single copies of NRC draft reports are available free, to the extent of supply, upon written request to the Division of Technical Information and Document Control, U.S. Nuclear Regulatory Commission, Washington, DC 20555.

Copies of industry codes and standards used in a substantive manner in the NRC regulatory process are maintained at the NRC Library, 7920 Norfolk Avenue, Bethesda, Maryland, and are available there for reference use by the public. Codes and standards are usually copyrighted and may be purchased from the originating organization or, if they are American National Standards, from the American National Standards Institute, 1430 Broadway, New York, NY 10018.

NUREG/CR-3886
ORNL/TM-9265

Distribution Category R5

ACTIVITY AND FLUENCE CALCULATIONS FOR THE STARTUP AND TWO-YEAR IRRADIATION EXPERIMENTS PERFORMED AT THE POOLSIDE FACILITY

R. E. Maerker and B. A. Worley
Engineering Physics and Mathematics Division
Oak Ridge National Laboratory
Oak Ridge, TN 37831

NRC Monitor: C. Z. Serpan
Engineering Technology Division

Project Manager: F. B. K. Kam
Oak Ridge National Laboratory

Manuscript Completed: August 1984

Date Published - October 1984

This Work Performed for
Nuclear Regulatory Commission
under
DOE Interagency Agreements 40-551-75 and 40-552-75
NRC FIN No. B0415

Prepared by the
Oak Ridge National Laboratory
Oak Ridge, Tennessee 37831
operated by
Martin Marietta Energy Systems, Inc.
for the
U.S. DEPARTMENT OF ENERGY
under contract No. DE-AC05-84OR21400

TABLE OF CONTENTS

LIST OF FIGURES

LIST OF TABLES

LIST OF TABLES (cont'd)

ABSTRACT

Fluence rate, fluence, and activity calculations are presented for each of three exposures (two surveillance capsules and a pressure vessel capsule) performed during the two-year metallurgical blind test experiment at the ORR-Poolside Facility in Oak Ridge. This experiment is intended to serve as an international metallurgical benchmark, and the spectral fluence calculations described in this report have been made available to the international community in pressure vessel dosimetry to be used in their damage assessment studies and/or adjustment procedures.

Following the same simplified calculational methods introduced and described in a reanalysis of the startup experiment, fission source distributions were obtained from 3-dimensional diffusion theory for most of the 52 cycles active during the course of the complete experiment, combined in small groups, and the resultant ex-core group fluxes calculated by two-dimensional discrete ordinate transport theory. Dosimeter activities at the end of each of the three irradiations were calculated by decaying the saturated activities obtained for each group of cycles and summing over the pertinent cycles. Calculations indicated that cycle-to-cycle variations of the saturated activities could be as much as 40%.

Comparisons of the dosimeter end-of-irradiation activities with HEDL measurements indicate agreement generally within 15% for the first surveillance capsule, 5% for the second, and 10% for three locations in the pressure vessel capsule, which are as good as if not somewhat better than comparisons in the startup experiment. The calculations thus validate the trend of the measurements in both the startup and the two-year experiments, and confirm the presence of a significant cycle-to-cycle variation in the core leakage. The tape containing the unadjusted spectral fluences for each of the three exposures that can be used in the metallurgical analysis is thus considered to be accurate to within about 10%.

REVISED STARTUP CALCULATIONS

The dosimeter saturated activities for the startup experiment performed at the PSF using cycle 151-A in the fall of 1979 have been recalculated. The original calculations, which have been documented (1,2), involved use of a DB^2 option in the DOT transport code (3) that provided modeling of the complication of the finite dummy simulated surveillance capsule (SSC) geometry (see Figs. 1 and 2). At the time the original calculations were made, it was believed that the streaming of the fast neutrons through the water surrounding the SSC could strongly influence the midplane fluence rates in the simulated pressure vessel capsule (SPVC). This belief was based, first, on the results of a DOT scoping calculation which indicated that fluence rate levels at the three midplane locations in the SPVC were about 40% too low if the SSC were simply represented as a slab of infinite height and width, and second, on the easily demonstrable fact that the transmission of neutrons above about 2 MeV through water is higher than through comparable thicknesses of steel. It was decided, therefore, to use the approach outlined in the papers referenced above. Although the theory employed was correct and should lead to accurate results whether streaming is important or not, the complicated manipulations of the leakage data required and approximations used in the cross section spatial weighting procedure did not lead to a high degree of confidence in the final calculated activities.

The new calculations were inspired by this growing dissatisfaction with the original calculations and by the fact that the importance of streaming through the water around the SSC on the midplane dosimeters seemed inconsistent with the results of a channel theory calculation that M. L. Williams had done and which showed no such importance (4). Furthermore, C. A. Baldwin had obtained what he considered to be satisfactory agreement between calculations and PCA measurements in a geometry similar to the present one without resorting to such a complicated procedure (5). A further consideration in performing the calculations was the desire that a simpler procedure than the original one might be found so that it could be applied to the analysis of the long term experiment. In case this latter application became necessary, the procedure would have to be repeated many times over the course of the experiment.

The "streaming" problem was thus reexamined in more detail than previously, and the conclusion was reached that, for detectors located in the pressure vessel near the midplane, there was little or no effect produced by the water (i.e., ~1%) (6). Subsequent calculations also indicated that the horizontal voids in the SSC and in the SPVC had a negligible effect on the midplane and near-midplane fluence rates (i.e., the 1-inch void in the SSC and the 1/4-inch voids in the SPVC do not influence the midplane fluence rates). Thus, the XY and YZ DOT calculations required in the fluence rate synthesis procedure (see the following) can be made completely independent of each other. For example, in regions where more than one material is present at the same radial location (SSC locations where void, steel and water occur and the SPVC where void and steel occur), the near midplane fluence rates will

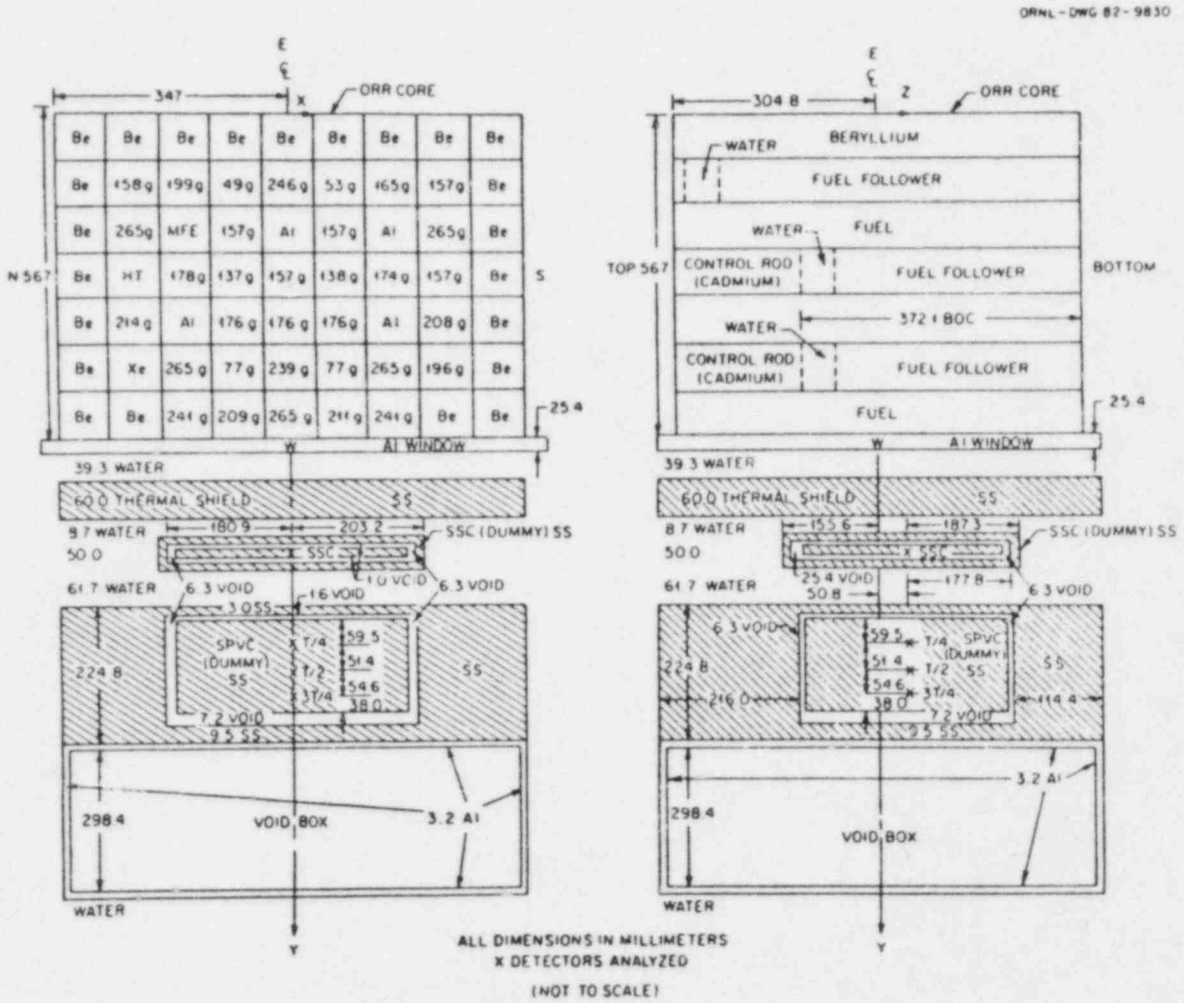

Fig. 1. Horizontal (XY) Cut at Location of Maximum Axial Flux of ORR-PSF Startup Experiment.

Fig. 2. Vertical (YZ) Cut at Location of Radial Centerline of ORR-PSF Startup Experiment.

not be changed if an infinitely high and wide steel slab is modeled in the calculation. This conclusion is consistent with everything except the results of the original scoping calculation previously described, which indicated that C/E values in the neighborhood of 0.6 would result if such a pair of calculations were used. However, these scoping calculations were based on a single XY run, the remaining YZ/Y factor being estimated from earlier PCA calculations; thus the resulting calculated activities were only approximately correct.

The results of these new calculations are presented below, where in addition to the complete decoupling of the XY and YZ calculations, the other change made from the previous calculations is the use of the ELXSIR cross section library (7) in place of the VITAMIN-C library. The same diffusion theory (VENTURE) fission source that was previously calculated was used (8). As in the previous calculations, only neutrons down to 100 Kev were considered, so that any subthreshold contributions to the $^{237}Np(n,f)$ activity from neutrons below 100 Kev were not calculated. The use of the ELXSIR library implies also the use of a revised set of ENDF/B-V dosimetry cross sections developed by Fu (9), which differ somewhat from the ENDF/B-V set used in the original calculation. The major differences in the two sets lie in the $^{27}A\ell(n,\alpha)$, $^{63}Cu(n,\alpha)$, and $^{46}Ti(n,p)$ reactions, the Fu set being about 5%, 9% and 4% lower than the ENDF/B-V set, respectively.

Table 1 contains a summary of all the results of the individual saturated activities from each of the three revised runs employing XY, YZ, and Y (ANISN) geometry. The combined results contain a reaction rate-and location-independent bias factor of 1.057 coming from three effects: 1.024 from a heterogeneous transport correction to the plate and water homogeneously mixed element representation of the core, 1.01 from a slightly inconsistent source normalization of the YZ DOT run relative to the Y ANISN run, and 1.022 from a renormalization of the neutron source in VENTURE using 7.71×10^{16} neutrons/sec per MW rather than 7.545×10^{16}. Thus, using the same fluence rate synthesis procedure as previously,

$$\phi_g(x,y,z) = \phi_g(x,y)\phi_g(y,z)/\phi_g(y) \quad , \tag{1}$$

leads to the following equation relating the bias-corrected combined saturated activities with the component activities calculated for each of the three runs:

$$RR = 1.057\ (Rxy)(Rzy/Ry)\ (Vy/VxyVyz) \ , \tag{2}$$

where the source for the XY calculation is the VENTURE XYZ source integrated over Z, the source for the YZ calculation is the VENTURE XYZ

Table 1. Component Saturated Activities, Combined Saturated Activities, and Comparison with Measurements*

	$^{63}Cu(n,\alpha)$	$^{46}Ti(n,p)$	$^{54}Fe(n,p)$	$^{58}Ni(n,p)$	$^{238}U(n,f)$	$^{237}Np(n,f)^{\dagger}$
SSC						
Rxy	2.521-13‡	4.818-12	3.870-11	5.294-11	2.091-10	1.637-9
Ryz	2.317-13	4.399-12	3.493-11	4.769-11	1.865-10	1.477-9
Ry	5.115-12	9.599-11	7.508-10	1.025-9	3.997-9	3.142-8
C,RR	2.58 -15**	5.00 -14	4.07 -13	5.57-13		
E,RR	3.07 -15**	6.12 -14	4.67 -13	6.45-13		
C/E	0.84	0.82	0.87	0.86		
T/4‡‡						
Rxy	2.531-14	4.354-13	3.149-12	4.344-12	1.793-11	1.745-10
Ryz	2.372-14	4.062-13	2.917-12	4.018-12	1.649-11	1.597-10
Ry	5.756-13	9.722-12	6.856-11	9.443-11	3.868-10	3.896-9
C,RR	1.90 -16	3.31 -15	2.44 -14	3.36 -14	1.39 -13	1.30 -12
E,RR	2.10 -16	4.04 -15	2.75 -14	3.90 -14	1.56 -13	1.40 -12
C/E	0.90	0.82	0.89	0.86	0.89	0.93
T/2‡‡						
Rxy	9.566-15	1.591-13	1.163-12	1.642-12	7.542-12	9.870-11
Ryz	9.009-15	1.494-13	1.085-12	1.531-12	6.998-12	9.115-11
Ry	2.225-13	3.638-12	2.598-11	3.668-11	1.681-10	2.326-9
C,RR	7.05 -17	1.19 -15	8.84 -15	1.25 -14		
E,RR	7.97 -17	1.47 -15	1.02 -14	1.49 -14		
C/E	0.88	0.81	0.87	0.84		
3T/4‡‡						
Rxy	3.396-15	5.447-14	3.983-13	5.765-13	2.902-12	4.984-11
Ryz	3.228-15	5.165-14	3.759-14	5.433-13	2.722-12	4.643-11
Ry	8.118-14	1.280-12	9.162-12	1.327-11	6.697-11	1.244-9
C,RR	2.46 -17	4.00 -16	2.97 -15	4.30 -15		
E,RR	2.81 -17	5.30 -16	3.74 -15	5.56 -15		
C/E	0.87	0.75	0.80	0.77		

*All measurements performed by ECN except $^{58}Ni(n,p)$ in the SSC which was performed by CEN/SCK.

†Neglecting the ~3% contribution below 100 Kev coming from subthreshold fission.

‡Read 2.521×10^{-13}. Units are reactions per atom per second integrated over the detector zone volume.

**Units are reactions per atom per second.

‡‡The symbols T/4, T/2, and 3T/4 refer to approximate one-quarter, one-half, and three-quarter depth locations into the pressure vessel.

source integrated over X, and the source for the Y calculation is the VENTURE XYZ source integrated over X and Z, and where the V's represent volumes of the detector zones used in the integration of the edited zone activities for each run. The factor 1.057 Vy/VxyVyz has the value 0.2263 for the SSC detector and the value 0.1820 for each of the three SPVC detectors (T/4, T/2, and 3T/4). It should be pointed out that Eq. (2) is not derivable from Eq. (1), but is an excellent (within 1%) approximation to activities calculated directly from Eq. (1). A further description of this approximation is given in the discussion of the long-term experiment analysis presented later.

The conclusion from this final set of comparisons is that the agreement is generally within 15% for the SSC, 10% for the T/4, 15% for the T/2 and 20% for the 3T/4 locations. This averages only about 5% better than the original calculations, but one has far more confidence in these latest results. It would seem that there is about a 10% underestimate of the ORR leakage calculated by VENTURE. In agreement with conclusions derived from the PCA confrontation (10) there is again an indication that the total iron inelastic cross sections from ENDF/B-IV used in the calculations are about 8% high.

References

1. Williams, M. L. and R. E. Maerker, "Calculations of the Startup Experiments at the Poolside Facility," Proc. Fourth ASTM-EURATOM Sym. on Reactor Dosimetry, NUREG/CP-0029, Vol. 1, CONF820321/V1 (1982).

2. Maerker, R. E. and M. L. Williams, Calculations of Two Series of Experiments Performed at the Poolside Facility Using the Oak Ridge Research Reactor, NUREG/CR-2696 ORNL/TM-8326 (1982).

3. Rhoades, W. A. and R. L. Childs, An Updated Version of the DOT4 One- and Two-Dimensional Neutron/Photon Transport Code, ORNL-5851 (1982).

4. Private Communication.

5. Private Communication.

6. Informal Intra-Laboratory Correspondence, R. E. Maerker to F.B.K. Kam (1983).

7. Williams, M. L., R. E. Maerker, W. E. Ford, III and C. C. Webster, The ELXSIR Cross Section Library for LWR Pressure Vessel Irradiation Studies, EPRI Report (to be published in 1984).

8. Vondy, D. R., T. B. Fowler and G. W. Cunningham, III, The Bold Venture Computation System for Nuclear Reactor Core Analysis, Version III, ORNL-5711 (1981).

References (cont'd)

9. Fu, C. Y. and D. M. Hetrick, "Experience in Using the Covariances of Some ENDF/B-V Dosimetry Cross Sections: Proposed Improvements and Addition of Cross-Reaction Covariances," Proc. Fourth ASTM-EURATOM Sym. on Reactor Dosimetry, NUREG/CP-0029, Vol. 2, CONF-820321/V2 (1982).

10. McElroy, W. N. (Ed.), LWR Pressure Vessel Surveillance Dosimetry Improvement Program: PCA Experiments and Blind Test, NUREG/CR-1861, HEDL-TME 80-87-R5 (1981).

TWO-YEAR IRRADIATION EXPERIMENT ANALYSIS

Introduction

Since some HEDL dosimetry measurements in the two-year irradiation experiment disagreed by ~10-20% with ECN and CEN/SCK measurements performed earlier for the startup experiment, (1,2,3), it is of interest to investigate analytically the cause of this disagreement. If due to differences in the measurement techniques between HEDL and the Europeans, that is one thing, and leads to its own worries and reevaluation of measurement uncertainties; if due to differences in the source distributions (i.e., cycle-to-cycle variations) or differences in the geometry of the two experiments, this should be verified and the original startup calculations replaced by more rigorous ones that take these differences into account. A further consideration from the authors' viewpoint is their choice of the startup experiment as an important benchmark in the LEPRICON adjustment procedure (4), and it is highly desirable that the startup calculations and use of ECN measurements are consistent with the additional information provided by the two-year experiment. A final consideration is that, because of the large number of calculations involved, probably no one else will perform them, and hence these calculations will be the only ones to be used in the analysis of the blind test metallurgical benchmark experiment for which the two-year irradiation sequence was designed.

In the previous section, the results of a simpler calculation of the startup experiment than the one originally performed were presented. Summarizing, the method adopted for this simpler calculation was based on the validated results of further calculations that showed there was no effect of streaming around the finite simulated surveillance capsule (SSC) on the near-centerline fluence rates in the SSC or the simulated pressure vessel capsule (SPVC). Furthermore, the presence of the horizontal voids such as the 1-inch cable storing void in the SSC and the 1/4-inch voids in the SPVC does not affect the near-centerline fluence rates. Thus the 3-dimensional fluence rate synthesis procedure involved using three calculations - DOT XY, DOT YZ and ANISN Y - in which the revised geometry assumed the SSC to be infinitely high and wide, and with the horizontal voids only affecting the YZ fluence rate profiles at axial distances greater than about ±13 cm from a horizontal plane 5.08 cm below the reactor centerline. This simplified method was used in all the transport calculations soon to be described in the two-year analysis as well; indeed, if it had been necessary to use the method involving XY and YZ bucklings originally adopted for the startup analysis, the cost and time involved would have been prohibitive. As it is, the discovery of the simpler method, which is just as accurate and less subject to data manipulation error, allowed the present analysis to be performed efficiently and accurately.

Irradiation History

The history of the two-year irradiation is presented in Table 2, where the data originally supplied was altered slightly to include the effects of setback in the duration of each cycle. Thus the column headed "Δtup" is simply t(retracted)-t(inserted), the column headed "setback" is the difference between Δtup and the "Delta-t" column in the original data which didn't include setback, and the column headed "average power including setback" replaces the "average power" column in the original data. In this way, the effects of setback, though small, have been included into the time history of the irradiation. The k_{eff} values in Table 2 are those calculated using VENTURE and a modified VIPOR in which the axial partially burned fuel profile correlations were renormalized whenever they went negative (5). It should be noted that only a middle-of-cycle VENTURE calculation was made for each cycle, the assumption being that the departure of the within-cycle source variation from linearity about the middle-of-cycle distribution is small compared to the cycle-to-cycle variation. The data and times in Table 2 given are assumed to include the ±1 hour adjustments from changing to daylight saving time and back to standard time. These adjustments are assumed to have occurred on October 26, 1980, April 26 and October 25, 1981 and April 25, 1982, all at 2 AM. No leap days occurred during the irradiation, so that the total elapsed time between the first insertion of the experiment and the last retraction was:

1980: 10.433+24(31+30+31+31+30+31+30+31)+1=5891.43 hrs
1981: 24(365)= 8760.00 hrs
1982: 24(31+28+31+30+31)+24(22)-1=4151.00 hrs,

for a total of 18802.43 hrs. This agrees within 0.22 hrs≈13 min. of the retraction time in cycle 161C relative to the insertion time in cycle 153B. This difference is completely negligible and not worth the trouble of tracing. It is to be noted that the irradiation consisted of 52 fuel cycles of which all but a few (155G, 155H, 156A, 156B) had VENTURE calculations performed for them. In addition to these four, VENTURE source distributions were not used for cycles 154H and 155D because they were late in being calculated and nominal distributions were used instead. The effect of using nominal source distributions for these six cycles instead of calculated ones should result in an estimated maximum uncertainty in the calculated fluences in the SPVC and simulated void box capsule (SVBC) locations (the only locations these cycles affect) of 2.4%, with somewhat smaller values for the calculated dosimeter activities. Hence no significant uncertainty is introduced into the analysis by the cavalier treatment of these six cycles.

Since it was subsequently discovered that the void box developed a leak early in the irradiation history, thus destroying the usefulness of the measured SVBC results, the analysis next to be described will not dwell on any of the details of the SVBC calculations which assumed void rather than water in the region between the rear of the pressure vessel and the VEPCO capsule.

Table 2. Irradiation History and Cycle Parameters

Cycle	k_{eff}	Time and Date Inserted		Time and Date Retracted		Down Time After Previous irradiation Δt_d (hrs)	t(inserted) (hrs)	t(retracted) (hrs)	Δtup (hrs)	setback Δt_s (hrs)	Average Power including setback(Mw)
						Start Irradiation of SSC-1, SPVC, and SVBC					
153B	1.0242	30-Apr-80	13:34	8-May-80	7:00		0	185.43	185.43	1.00	29.822
153C	1.0251	8-May-80	16:43	14-May-80	13:30	9.72	195.14	335.90	140.76	0	29.800
153C	1.0251	16-May-80	9:57	21-May-80	2:17	44.45	380.35	492.68	112.33	0	29.957
153D	1.0162	22-May-80	10:49	6-June-80	24:00	32.53	525.21	898.39	373.18	2.55	29.657
153F	1.0224	12-June-80	9:20	23-June-80	12:55	129.33	1027.72	1295.30	267.58	0.43	29.377
						End Irradiation of SSC-1					
153G	1.0042	27-June-80	18:30	5-July-80	3:30	101.58	1396.88	1573.88	177.00	2.32	28.855
153G	1.0042	7-July-80	13:55	8-July-80	9:40	58.42	1632.30	1652.05	19.75	0.18	29.058
153G	1.0042	8-July-80	15:18	13-July-80	8:00	5.63	1657.68	1770.38	112.70	1.01	29.565
154A	1.0047	18-July-80	17:00	18-July-80	18:32	129.00	1899.38	1900.70	1.32	0.82	3.712
154A	1.0047	18-July-80	22:50	21-July-80	4:26	4.30	1905.00	1958.60	53.60	1.26	28.319
154A	1.0047	22-July-80	05	31-July-80	7:00	29.65	1988.25	2201.17	212.92	13.39	28.200
154B	1.0066	31-July [illegible]	20	12-Aug-80	19:02	11.33	2212.50	2501.20	288.70	0.33	30.335
154C	1.0019	15-Aug-80	[illegible]	15-Aug-80	16:07	67.77	2568.97	2570.29	1.32	0.05	28.977
154D	1.0024	21-Aug-80	[illegible]	26-Aug-80	16:00	138.80	2709.09	2834.17	125.08	0.39	28.849
154E	1.0016	27-Aug-80	14:30	1-Sept-80	3:29	22.50	2856.67	2965.62	108.95	0	29.799
154E	1.0016	3-Sept-80	[illegible]	9-Sept-80	6:00	54.40	3020.02	3162.14	142.12	0.57	30 031
154F	1.0007	10-Sept-80		23-Sept-80	4:00	27.37	3189.51	3494.14	304.63	1.73	29 471
154G	.9993	23-Sept-80	13:52	5-Oct-80	21:32	9.87	3504.01	3799.68	295.67	0.44	29.909
154H	1.0190	7-Oct-80	13:45	27-Oct-80	17:50	40.23	3839.91	4083.95	244.04	0	29.905
154I	.9858	21-Oct-80	12:48	29-Oct-80	4:00	90.97	4174.92	4359.05	184.13	1.00	29.486
154J	.9890	29-Oct-80	18:47	8-Nov-80	8:00	14.78	4373.83	4603.05	229.22	0.29	29.223
155B	.9983	3-Dec-80	14:51	9-Dec-80	0:26	606.85	5209.90	5339.48	129.58	0.90	28.786
155C	.9920	10-Dec-80	12:54	18-Dec-80	5:15	36.47	5375.95	5560.30	184.35	0	28.247
155D	.9936	18-Dec-80	17:46	30-Dec-80	8:00	12.52	5572.82	5851.59	278.77	0.54	27.832
155E	.9891	30-Dec-80	16:11	7-Jan-81	8:00	8.18	5859.77	6043.59	183.82	0.29	26.823
155F	.9922	7-Jan-81	21:55	15-Jan-81	4:00	13.92	6057.51	6231.59	174.08	0.22	27.115
155G		16-Jan-81	11:41	19-Jan-81	20:22	31.68	6263.27	6343.95	80.68	0.21	30.066
155H		21-Jan-81	9:02	22-Jan-81	7:16	36.67	6380.62	6402.85	22.23	0.89	29.311
155H		22-Jan-81	16:18	2-Feb-81	8:00	9.03	6411.88	6667.58	255.70	0.61	30.346
156A		9-Feb-81	13:35	24-Feb-81	8:00	173.58	6841.16	7195.58	354.42	2.92	27.279
156B		24-Feb-81	15:00	13-Mar-81	8:04	7.00	7202.58	7603.65	401.07	2.19	27.223
156B		13-Mar-81	8:47	16-Mar-81	7:00	0.72	7604.37	7670.59	66.22	0.61	27.168
156C	1.0052	19-Mar-81	10:13	30-Mar-81	22:40	79.22	7749.81	8026.26	276.45	0	30.447
156C	1.0052	31-Mar-81	11:33	2-Apr-81	4:00	12.88	8039.14	8079.59	40.45	1.08	29.598
156D	1.0076	2-Apr-81	16:10	19-Apr-81	8:00	12.17	8091.76	8491.60	399.84	0	30.290
157A	1.0021	27-Apr-81	11:12	11-May-81	3:12	194.20	8585.80	9013.80	328.00	2.50	30.174
157B	1.0184	11-May-81	17:24	27-May-81	4:00	14.20	9028.00	9398.60	370.60	0	30.335

Table 2. (cont'd)

Cycle	k_{eff}	Time and Date Inserted		Time and Date Retracted		Down Time After Previous irradiation Δt_d (hrs)	t(inserted) (hrs)	t(retracted) (hrs)	Δtup (hrs)	setback Δt_s (hrs)	Average Power including setback(Mw)
						Start Irradiation of SSC-2					
157C	1.0166	29-May-81	11:39	29-May-81	20:45	55.65	9454.25	9463.35	9.10	0	30.048
157C	1.0166	1-June-81	11:49	9-June-81	8:10	63.07	9526.42	9714.77	188.35	0.94	29.997
157D	1.0127	10-June-81	8:15	23-June-81	4:23	24.08	9738.85	10046.98	308.13	0	30.352
157E	.9756	25-June-81	12:20	10-July-81	12:00	55.95	10102.93	10462.60	359.67	0	30.044
158C	1.0018	22-July-81	13:47	6-Aug-81	6:30	289.78	10752.38	11105.10	352.72	0.15	27.082
158D	.9997	7-Aug-81	19:05	20-Aug-81	4:00	36.58	11141.68	11438.61	296.93	0	27.008
158E	1.0101	21-Aug-81	15:17	30-Aug-81	24:00	35.28	11473.89	11698.61	224.72	0	30.354
158F	1.0076	2-Sept-81	19:01	8-Sept-81	16:52	67.02	11765.63	11907.48	141.85	0.22	30.136
158G	1.0274	11-Sept-81	8:17	25-Sept-81	2:00	63.42	11970.90	12300.62	329.72	0	30.260
						End Irradiation of SSC-2					
158H	1.0126	25-Sept-81	23:10	13-Oct-81	3:20	21.17	12321.79	12733.96	412.17	0.12	30.180
158I	1.0206	13-Oct-81	20:30	23-Oct-81	3:00	17.17	12751.13	12973.63	222.50	0.57	30.174
158J	1.0142	23-Oct-81	13:28	26-Oct-81	20:13	10.47	12984.10	13063.85	79.75	0.12	29.819
158J	1.0142	27-Oct-81	9:41	4-Nov-81	4:00	13.47	13077.32	13263.64	186.32	1.43	30.267
158K	1.0173	4-Nov-81	16:10	15-Nov-81	8:00	12.17	13275.81	13531.64	255.83	0.09	30.311
159A	1.0156	24-Nov-81	14:12	12-Dec-81	6:00	222.20	13753.84	14177.64	423.80	0	30.287
159B	1.0037	18-Dec-81	9:47	28-Dec-81	13:20	147.78	14325.42	14568.97	243.55	0.43	30.009
159C	1.0054	31-Dec-81	21:21	6-Jan-82	8:36	80.02	14648.99	14780.24	131.25	0.71	29.794
159C	1.0054	6-Jan-82	14:18	14-Jan-82	3:00	5.70	14785.94	14966.64	180.70	0.37	30.234
159D	1.0121	21-Jan-82	15:36	1-Feb-82	2:58	180.60	15147.24	15398.61	251.37	0	30.256
159E	1.0025	1-Feb-82	16:56	7-Feb-82	8:00	13.97	15412.58	15547.65	135.07	0	30.126
160A	1.0020	12-Feb-82	17:33	18-Feb-82	9:00	129.55	15677.20	15812.65	135.45	0.07	29.987
160B	1.0064	18-Feb-82	18:59	8-Mar-82	8:20	9.98	15822.63	16243.98	421.35	0.14	30.173
160C	1.0175	9-Mar-82	15:33	25-Mar-82	3:00	31.22	16275.20	16646.65	371.45	1.44	30.113
160D	1.0166	26-Mar-82	18:55	5-Apr-82	3:00	39.92	16686.57	16910.65	224.08	0.34	30.223
160E	1.0108	5-Apr-82	18:40	16-Apr-82	15:05	15.67	16926.32	17186.74	260.42	0.69	29.856
161B	1.0149	29-Apr-82	17:42	24-May-82	3:30	313.62	17500.36	18086.16	585.80	0.88	30.062
161C	1.0223	27-May-82	22:28	22-June-82	24:00	90.97	18177.13	18802.66	625.53	1.73	30.116
						End Irradiation of SPVC and SVBC					

Method of Calculation

The sequence of calculations in the VENTURE-DOT method is shown in Fig. 3, where the introduction of the source combining procedure over groups of cycles allows one to perform a single DOT calculation (actually two, an XY and a YZ) for a group of cycles, rather than for each individual cycle, thus cutting down significantly the cost and time of the analysis. The source combining should not include too many cycles at a time or the variation from cycle to cycle, if significant, would be almost lost. For this type of analysis, where as much of the (unknown) source time variation should be retained as possible within the limiting framework of the costly DOT calculations, it was decided to do little or no combining of cycles near the end of an irradiation period (i.e., cycles active immediately prior to the removals of the SSC-1, the SSC-2, and the SPVC and SVBC), to allow a more accurate calculation of the shorter-lived dosimeter activities at the end of irradiation. For the longer-lived activities as well as for the shorter-lived ones several half-lives removed in time, the cycle sources may be combined in ever increasing groups of cycles. For the fluence calculation no decay complications need to be considered, so that if it weren't for the dosimetry considerations all the cycle sources active during a given irradiation period (i.e., SSC-1, SSC-2, or SPVC + SVBC exposures) could be combined and only one pair of DOT calculations performed for each. The combining was based on weighting each cycle by its average power (each VENTURE calculation was normalized to 30 MW), duration, and calculated k_{eff}:

$$\bar{S}_G = 1.0225 \left[\sum_{i=1}^{L(G)} \left(\frac{S_i}{k_{eff}}\right)\left(\frac{\bar{P}_i}{30}\right) \Delta tup(i) \right] / \left[t_L^G(\text{retracted}) - t_1^G(\text{inserted}) \right] . \quad (3)$$

In Eq. (3), the symbols $\bar{S}_G$ and S_i represent the combined and individual cycle sources as function of either x and y, y and z, or y, depending on which transport calculation is to be made. The factor 1.0225 represents a renormalization of the VENTURE neutron source to reflect updated information on $(\bar{\nu}/K)$; the denominator represents the total time interval that the group of cycles represents the core source, and includes the down time between each cycle $\Delta t_d(i)$. One is thus replacing L different sources, each active for $\Delta tup(i)$, by a single reduced source of extended duration $\sum[\Delta tup(i) + \Delta t_d(i)] = t_L$ (retracted) $-t_1$ (inserted). If one chooses the group of cycles such that $\Delta t_d(i) \ll \Delta tup(i)$ for all i in the group, the decay can be very accurately calculated as coming from a constant source $\bar{S}_G$ extending over the period represented by the denominator of Eq. (3). If a particularly large down time occurred, the group was terminated with the cycle immediately preceding, so that all cycle sources in the group are properly decayed through this common down time interval. A case in point is cycle 158C in the SSC-2 irradiation (see Table 2); there was a

ORNL DWG.84-9508

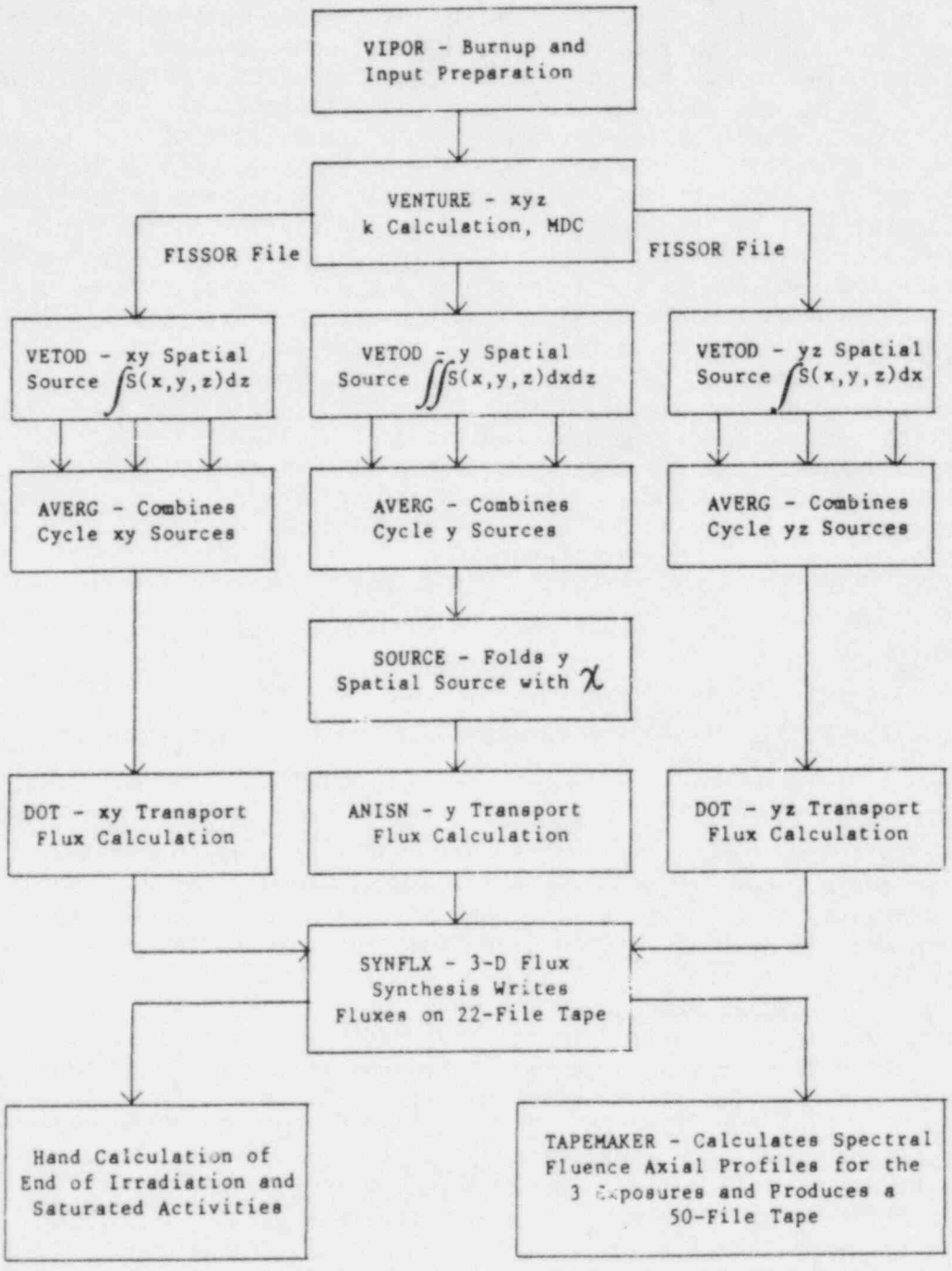

Fig. 3. Sequence of Calculations

delay of 289.78 hrs after cycle 157E before cycle 158C commenced. Thus if one were to combine the sources from any cycles before 158C with those after 157E, the decay based on the combining procedure illustrated by Eq. (3) would be somewhat overcalculated for cycle 158C and any cycles in the group occurring after 158C. Thus a natural dividing line separating the groups occurs between cycles 157E and 158C. Table 3 illustrates the grouping of the cycles used in this analysis together with the various weights for each cycle.

The component fluence rates calculated in each of the two DOT runs as well as in the ANISN run were synthesized in a manner completely analogous to the procedure followed in the startup experiment analysis,

$$\phi_g^G(x,y,z) = \phi_g^G(x,y)\phi_g^G(y,z)/\phi_g^G(y) \quad . \tag{4}$$

These synthesized fluence rates were calculated as axial profiles for specific values of x and y for each group of cycles appearing in Table 3. Fluence rates were calculated using the same ELXSIR library as was used in the startup analysis, and were followed down only to 0.098 Mev (i.e., only the first 38 groups of the library were used). These fluence rates were then multiplied by the total duration of the group, t_L(retracted)-t_1(inserted), which includes the intercycle down times if any, and summed over all the cycle groups to yield the spectral fluences,

$$\Phi_g(x,y,z) = 1.039 \sum_G \phi_g^G(x,y,z)\,[t_L^G(\text{retracted}) - t_1^G(\text{inserted})] \quad , \tag{5}$$

where the factor 1.039 represents an energy- and spatially-independent bias factor that accounts for the combined effects of the plate and water fuel element geometry and of a slightly inconsistent normalization between the DOT YZ and ANISN Y sources.

These spectral fluence axial profiles appear on tape X13850 in fifty files for possible use in spectral adjustment codes and/or analysis of the metallurgical specimens. A complete description of the contents of this tape is relegated to the appendix.

Calculations of the measured dosimeter activities were made as both saturated activities from each cycle group as well as decayed end of irradiation activities.

Saturated activities for the $^{63}Cu(n,\alpha)$, $^{46}Ti(n,p)$, $^{54}Fe(n,p)$, and $^{58}Ni(n,p)$ dosimeters as well as the $^{238}U(n,f)$ and $^{237}Np(n,f)$ fission dosimeters were calculated for each cycle group by synthesizing the activities calculated in each of the transport runs,

$$RR_S^d(x,y,z) = [RR_S^d(x,y)RR_S^d(y,z)/RR_S^d(y)] \times [Vy/VxyVyz] \quad , \tag{6}$$

Table 3. Cycle Group Combinations and Reduced Individual Cycle Weights

Group		Cycles	$\frac{t_L(\text{retracted}) - t_l(\text{inserted})}{\sum_i \Delta tup(i)}$	Source Combination
1	SSC-1	153B+153C	1.124	$0.37352S_{153B}+0.51017S_{153C}$
2		153D	1.0	$0.99471S_{153D}$
3		153F	1.0	$0.97786S_{153F}$
4		153G-154C	1.353	$0.26071S_{153G}+0.21761S_{154A}+0.25271S_{154B}+0.00111S_{154C}$
5		154D-154J	1.159	$0.08626S_{154D}+0.15650S_{154E}+0.18293S_{154F}+0.18073S_{154G}+0.12059S_{154I}+0.14337S_{154J}$*
6		155B-155F	1.075	$0.18977S_{155B}+0.24024S_{155C}+0.23141S_{155E}+0.22383S_{155F}$†
7		155G-156B**	1.192	$0.50812\overline{S}_{155B-155F}+0.46452\overline{S}_{156C-157B}$**
8		156C-157B	1.165	$0.19772S_{156C}+0.24847S_{156D}+0.20416S_{157A}+0.22820S_{157B}$
9		157C-157E	1.165	$0.19695S_{157C}+0.31216S_{157D}+0.37439S_{157E}$
10	SSC-2	158C+158D	1.056	$0.47356S_{158C}+0.39838S_{158D}$
11		158E-158G	1.187	$0.27840S_{158E}+0.17491S_{158F}+0.40036S_{158G}$
12		158H-158K	1.046	$0.34607S_{158H}+0.18532S_{158I}+0.22270S_{158J}+0.21474S_{158K}$
13		159A-159C	1.239	$0.35518S_{159A}+0.20464S_{159B}+0.26202S_{159C}$
14		159D-160C	1.141	$0.17081S_{159D}+0.09227S_{159E}+0.09214S_{160A}+0.28715S_{160B}+0.24989S_{160C}$
15		160D+160E	1.032	$0.45395S_{160D}+0.52416S_{160E}$
16		161B	1.0	$1.0096S_{161B}$
17		161C	1.0	$1.0041S_{161C}$

*S_{154H} assumed to be $(S_{154D}+S_{154E}+S_{154F}+S_{154G}+S_{154I}+S_{154J})/6$
†S_{155D} assumed to be $(S_{155B}+S_{155C}+S_{155E}+S_{155F})/4$
**$S_{155G-156B}$ assumed to be $0.5\ (28.15/27.7)\overline{S}_{155B-155F}+0.5(28.15/30.3)\overline{S}_{156C-157B}$

where the last term represents the inverse of the volumes used in the integration of the edited saturated activities. These synthesized saturated activities are easily extracted from the region edits of the transport runs, and agree to within negligible error of the activities calculated using Eq. (4) in conjunction with folding with the reaction cross section,

$$RR_S^d(x,y,z) = \sum_g \phi_g(x,y,z)\sigma_g^d \quad . \tag{7}$$

Thus synthesizing the activities by using Eq. (6) is an excellent approximation to Eq. (7) and is more readily performed. Hence for a given group of cycles G,

$$RR_S^d = 1.039 \frac{t_L^G(\text{retracted}) - t_1^G(\text{inserted})}{\sum_i^{L(G)} \Delta tup(i)} \times [RR_S^d(x,y)RR_S^d(y,z)/RR_S^d(y)] \times [Vy/VxyVyz] \ , \tag{8}$$

where the time factor represents a correction to the original source combining prescription, Eq. (3), in order to properly renormalize the source and to provide a correct saturated activity.

These saturated activities are excellent indicators of the magnitude of any cycle-to-cycle variation, which is one of the most important questions to be answered by this analysis. Table 4 presents comparison of

Table 4. Cycle Group-to-Cycle Group Variation of Some Saturated Activities at the T/2 Location, x=-53.7, y=337.8, z=-8.5 mm

Cycles	Capsules Irradiated	$^{54}Fe(n,p)$	$^{63}Cu(n,\alpha)$	$^{237}Np(n,f)$	Np/Cu
153B+153C	SSC-1+	7.59-15*	5.87-17	6.17-13	1.05+4
153D	SPVC+	7.58-15	5.87-17	6.16-13	1.05+4
153F	SVBC	7.38-15	5.71-17	5.99-13	1.05+4
153G-154C		7.83-15	6.05-17	6.35-13	1.05+4
154D-154J	SPVC	7.47-15	5.79-17	6.06-13	1.05+4
155B-155F	+	9.15-15	7.06-17	7.42-13	1.05+4
156C-157B	SVBC	8.65-15	6.68-17	6.99-13	1.05+4
157C-157E	SSC-2+	8.82-15	6.80-17	7.14-13	1.05+4
158C+158D	SPVC+	9.65-15	7.45-17	7.83-13	1.05+4
158E-158G	SVBC	8.24-15	6.36-17	6.64-13	1.04+4
158H-158K		8.14-15	6.33-17	6.50-13	1.03+4
159A-159C	SPVC	8.42-15	6.54-17	6.73-13	1.03+4
159D-160C	+	7.83-15	6.10-17	6.24-13	1.02+4
160D+160E	SVBC	7.27-15	5.69-17	5.76-13	1.01+4
161B		7.14-15	5.62-17	5.65-13	1.01+4
161C		6.86-15	5.40-17	5.41-13	1.00+4
Startup(151A)	SSC+SPVC	8.84-15	7.05-17	7.04-13	1.00+4

*Read 7.59×10^{-15} reactions per atom per second at 30 MW, etc.

these saturated activities, corrected to a power of 30 MW, at the same T/2 location, together with the corresponding startup values. The coordinate system defining the x,y,z values appears in Fig. 4.

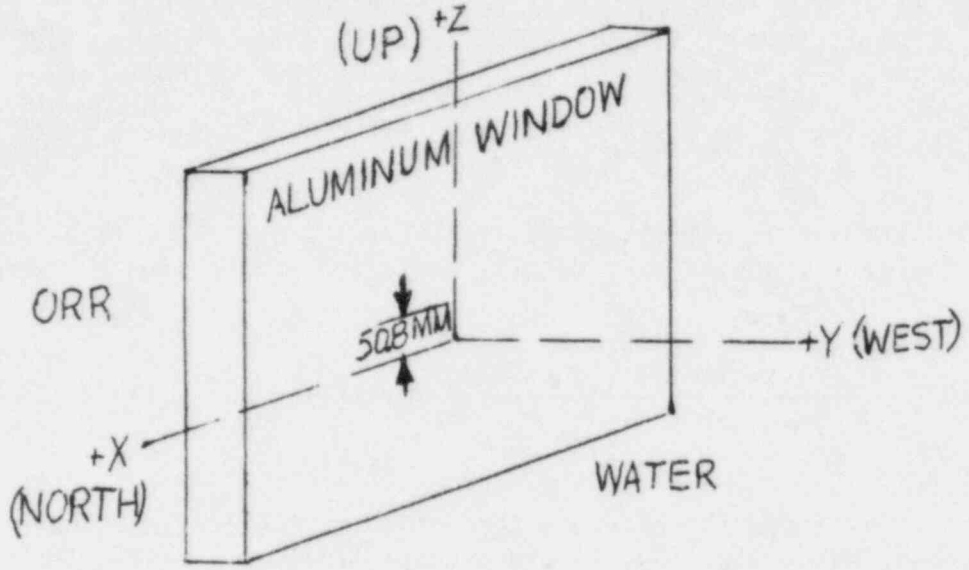

Fig. 4. Definition of the Cartesian Coördinate System. The Origin is Located 50.8mm below the Reactor Horizontal Midplane on the Outside Surface of the Aluminum Window.

Table 4 indicates that the variation is as much as 40%, with cycle groups 158C+158D and 161C representing the extremes. The spectrum remains essentially unaltered from cycle to cycle, however, since the last column represents the ratio of two markedly different responses. Further studies have shown that the constancy of the spectral shape with cycle at a given detector location remains valid for all such locations in the pressure vessel inward to and including the surveillance capsule. The spectral shapes are thus time-independent but remain space dependent. The rms standard deviation of the intensity at T/2 is about 10%. The straight averages of the two-year activities in Table 4 are 8.00-15, 6.21-17, and 6.44-13 respectively - about 10% lower than the startup activities. Thus it seems indicated that the differences in the HEDL and ECN measurements noted earlier for the two-year irradiation experiment and the startup experiment respectively are due to source variations and not differences in measurement techniques or water gap thicknesses.

Calculated Results and Comparisons with Measurements

To compare calculated activities with measurement, recourse must be made to decaying the saturated activities from each cycle group to the ends of irradiation, and summing over all pertinent cycle groups. Thus, for each dosimeter,

$$A_{EOI}(x,Y,z) = \sum_{G} \left[\frac{RR_S^G(x,y,z) \sum_{i=1}^{L(G)} \Delta tup(i)}{t_L^G(\text{retracted}) - t_I^G(\text{inserted})}\right] \times Y \times$$

$$\times \left[e^{-\frac{0.69315}{\tau_{1/2}}(t_{EOI}-t_L^G)} - e^{-\frac{0.69315}{\tau_{1/2}}(t_{EOI}-t_I^G)}\right] , \quad (9)$$

where Y is the yield of the reaction product. Notice the "up" time fraction factor in Eq. (9) is needed to reestablish the reduced fluence rate levels over the extended periods of time expressed by Eq. (5). In Eq. (9), $\tau_{1/2}$ is the half life of the decaying reaction product in days and the $(t_{EOI}-t^G)$ values must also be expressed in days. Table 5 shows the decay factors (i.e., the last bracket in Eq. (9)) calculated for the cycle groups in Table 4 for the end of SSC-1 irradiation.

Tables 6-8 present the results of the calculations using Eq. (9) and comparisons with some of the measurements as reported by HEDL for the SSC-1 irradiation (6).

Table 5. Decay Factors to the End of SSC-1 Irradiation for the Various Cycle Groups

	$\tau_{1/2}$(days)*	Y*	153B+153C	153D	153F
$^{63}Cu(n,\alpha)$	1925	1.0	.007275	.005549	.004006
$^{46}Ti(n,p)$	83.85	1.0	.1184	.1052	.08805
$^{54}Fe(n,p)$	312.5	1.0	.04133	.03268	.02443
$^{58}Ni(n,p)$	70.85	1.0	.1312	.1200	.1033
$^{238}U(n,f)^{137}Cs$	11023	.06000	.001287	.000976	.000701
$^{238}U(n,f)^{95}Zr$	64.10	.05105	.1387	.1294	.1136
$^{238}U(n,f)^{103}Ru$	39.43	.06229	.1683	.1788	.1780
$^{238}U(n,f)^{140}Ba$	12.79	.05948	.1096	.2323	.4535
$^{237}Np(n,f)^{137}Cs$	11023	.06267	.001287	.000976	.000701
$^{237}Np(n,f)^{95}Zr$	64.10	.05699	.1387	.1294	.1136
$^{237}Np(n,f)^{103}Ru$	39.43	.05584	.1683	.1788	.1780
$^{237}Np(n,f)^{140}Ba$	12.79	.05489	.1096	.2323	.4535

*Values are the ones used by HEDL in their data reduction procedures. (i.e., ENDF/B-V).

Table 6. Contributions of the Cycle Groups to the Calculated SSC-1 Activities at the End of Irradiation and Comparison with HEDL Measurements

		Axial Profiles at x = 0, y = 131.5 mm*					
		E_{EOI}	153B+153C	153D	153F	C_{EOI}	C/E
$^{54}Fe(n,p)$:	z= 122.2mm†	3.70-14‡	1.30-14	1.14-14	0.82-14	3.26-14	0.88
	z= 62.0	4.06-14	1.44-14	1.26-14	0.91-14	3.61-14	0.89
	z= -1.5	4.01-14	1.46-14	1.29-14	0.93-14	3.68-14	0.92
	z= -65.0	3.87-14	1.41-14	1.24-14	0.90-14	3.55-14	0.92
	z=-125.3†	3.36-14	1.25-14	1.10-14	0.80-14	3.15-14	0.94
$^{58}Ni(n,p)$:	z= 122.2mm†	1.86-13	0.57-13	0.57-13	0.48-13	1.62-13	0.87
	z= 62.0	2.01-13	0.63-13	0.64-13	0.53-13	1.80-13	0.90
	z= -1.5	2.04-13	0.64-13	0.65-13	0.54-13	1.83-13	0.90
	z= -65.0	1.95-13	0.61-13	0.62-13	0.52-13	1.75-13	0.90
	z=-125.3†	1.73-13	0.55-13	0.55-13	0.46-13	1.56-13	0.90
$^{46}Ti(n,p)$:	z= 122.2mm†	1.51-14	0.46-14	0.45-14	0.36-14	1.27-14	0.84
	z= 62.0	1.63-14	0.51-14	0.50-14	0.40-14	1.41-14	0.87
	z= -1.5	1.68-14	0.51-14	0.51-14	0.41-14	1.43-14	0.85
	z= -65.0	1.58-14	0.50-14	0.49-14	0.40-14	1.39-14	0.88
	z=-125.3†	1.35-14	0.43-14	0.43-14	0.35-14	1.21-14	0.90

*All locations are referred to the coördinates defined by HEDL.
†The calculations for the z=122.2mm location were actually performed for z=96.9mm and those for z=-125.3mm actually performed for z=-100.0mm, and were approximately corrected for the measurement location. These corrections amounted to approximately five and six percent decreases respectively.
‡Units are disintegrations per second per atom. Read 3.70×10^{-14}, etc.

Table 7. Contributions of the Cycle Groups to Additional Calculated SSC-1 Activities at the End of Irradiation and Comparison with HEDL Measurements

	(x,y,z)mm*	E_{EOI}	153B+153C	153D	153F	C_{EOI}	C/E
$^{54}Fe(n,p)$:	(-50,133,0)	3.92-14†	1.31-14	1.16-14	0.84-14	3.41-14	0.84
	(+50,133,0)	3.92-14	1.37-14	1.20-14	0.87-14	3.44-14	0.88
	(+40,139.9,-67.5)‡	3.21-14	1.16-14	1.02-14	0.74-14	2.92-14	0.91
$^{46}Ti(n,p)$:	(-39,133,0)**	1.67-14	0.46-14	0.46-14	0.37-14	1.29-14	0.77
	(+39,133,0)**	1.68-14	0.48-14	0.47-14	0.38-14	1.33-14	0.79
$^{58}Ni(n,p)$:	(-50,133,0)	1.98-13	0.57-13	0.58-13	0.49-13	1.64-13	0.83
	(+50,133,0)	2.01-13	0.60-13	0.61-13	0.51-13	1.72-13	0.86
	(+50,139.9,-67.5)	1.63-13	0.48-13	0.49-13	0.41-13	1.38-13	0.85
$^{63}Cu(n,\alpha)$:	(-50,133,0)	4.46-17	1.45-17	1.24-17	0.87-17	3.56-17	0.80
	(+50,133,0)	4.48-17	1.52-17	1.29-17	0.90-17	3.71-17	0.83
	(+42,139.9,-67.5)‡	3.64-17	1.24-17	1.06-17	0.75-17	3.05-17	0.84

*See Table 6.
†See Table 6.
‡Calculations were performed for the location (+50,139.9,-67.5). No corrections to the measured locations were made.
**Calculations were performed for the location (±50,133.0,0.0). No corrections to the measured locations were made.

Table 8. Contributions of the Cycle Groups to the Calculated SSC-1 Fission Product Activities at the End of Irradiation and Comparison with HEDL Measurements

	(x,y,z)mm*	E_{EOI}†	153B+153C	153D	153F	C_{EOI}	C/E
$^{238}U(n,f)^{137}Cs$:	(-45,133,-8.5)‡	4.08-16**	1.34-16	1.14-16	0.79-16	3.27-16	0.80
	(45,133,-8.5)	4.00-16	1.40-16	1.18-16	0.82-16	3.40-16	0.85
$^{238}U(n,f)^{95}Zr$:	(-45,133,-8.5)	4.40-14	1.23-14	1.28-14	1.08-14	3.59-14	0.82
	(45,133,-8.5)	4.30-14	1.28-14	1.33-14	1.13-14	3.74-14	0.87
$^{238}U(n,f)^{103}Ru$:	(-45,133,-8.5)	7.79-14	1.82-14	2.21-14	2.07-14	6.10-14	0.78
	(45,133,-8.5)	7.61-14	1.89-14	2.29-14	2.16-14	6.34-14	0.83
$^{238}U(n,f)^{140}Ba$:	(-45,133,-8.5)	1.07-13	0.11-13	0.27-13	0.50-13	8.8 -14	0.82
	(45,133,-8.5)	1.04-13	0.12-13	0.28-13	0.53-13	9.3 -14	0.89
$^{237}Np(n,f)^{137}Cs$:	(-43,133,7.4)	3.29-15	1.07-15	0.91-15	0.63-15	2.61-15	0.79
$^{237}Np(n,f)^{95}Zr$:	(-43,133,7.4)	3.75-13	1.05-13	1.09-13	0.93-13	3.07-13	0.82
$^{237}Np(n,f)^{103}Ru$:	(-43,133,7.4)	5.18-13	1.25-13	1.48-13	1.42-13	4.15-13	0.80
$^{237}Np(n,f)^{140}Ba$:	(-43,133,7.4)	8.04-13	0.80-13	1.89-13	3.56-13	6.25-13	0.78

*See Table 6.
†The $^{238}U(n,f)X$ measurements have not been corrected for possible effects of ^{239}Pu burn-in. (See Text).
‡The calculations were performed for the locations (±50,133.0,-7.9) for the ^{238}U fission product activities and (-50,133.0,7.9) for the ^{237}Np fission product activities. No corrections to the measured locations were made.
**See Table 6.

The slight differences in vertical or crosswise locations of the measured and calculated activities that are compared in these and succeeding tables have little or no effect on the comparisons (at most several percent in the case of the axial profiles in Tables 6 and 10).

A general conclusion from inspection of Tables 6-8 is that the agreement between calculation and measurement is within about 15%, which is about the same as the comparisons in the startup experiment. Since the SSC-1 measurements averaged about 10% lower than the startup ones, we have verified that this difference is due to source variations over the duration of the two experiments, and not to geometric differences or differences in the measurement techniques between ECN and HEDL. The axial profiles are well calculated, but there is evidence from Table 6 that the fluence rate synthesis procedure is beginning to underestimate at 12 cm above the y axis (~7 cm above the horizontal midplane). The calculated $^{46}Ti(n,p)$ activities are generally a little low, a circumstance noted in previous analyses. Finally, the effect of the decay on relative importance of each cycle group is clearly indicated in the tables, especially Table 8. Here it is apparent that the last cycle (153F) is becoming more and more important in its relative contribution to the end of irradiation activities as the half life decreases; indeed, it contributes better than half of the calculated ^{140}Ba activity ($\tau_{1/2}$ = 12.79 days) whereas only about a fourth of the ^{137}Cs activity ($\tau_{1/2}$ = 11023 days).

Following an identical analysis of the end of irradiation measurements for the SSC-2, (6), the next four tables, Tables 9-12, summarize similar results to those in Tables 5-8 for the SSC-1 exposures.

Table 9. Decay Factors to the End of SSC-2 Irradiation for the Various Cycle Groups

	157C-157E	158C+158D	158E-158G
$^{63}Cu(n,\alpha)$	.01464	.01014	.01236
$^{46}Ti(n,p)$	.1558	.1565	.2479
$^{54}Fe(n,p)$	.07499	.05667	.07345
$^{58}Ni(n,p)$	.1593	.1717	.2861
$^{237}Np(n,f)^{137}Cs$*	.002626	.001792	.002164
$^{237}Np(n,f)^{95}Zr$*	.1595	.1804	.3110
$^{237}Np(n,f)^{103}Ru$*	.1359	.2101	.4542

*Decay factors for $^{238}U(n,f)X$ are of course identical to those for $^{237}Np(n,f)X$.

Table 10. Contribution of the Cycle Groups to the Calculated SSC-2 Activities at the End of Irradiation and Comparison with HEDL Measurements

		Axial Profiles at x = 0,y = 131.5 mm*					
		E_{EOI}	157C-157E	158C+158D	158E-158G	C_{EOI}	C/E
$^{54}Fe(n,p)$:	z = 122.2mm†	7.09-14‡	2.58-14	2.12-14	2.22-14	6.92-14	0.98
	z = 62.0	7.74-14	2.90-14	2.36-14	2.52-14	7.78-14	1.01
	z = -1.5	7.97-14	2.96-14	2.37-14	2.67-14	8.00-14	1.00
	z = -65.0	7.63-14	2.86-14	2.27-14	2.62-14	7.75-14	1.02
	z = -125.3†	6.53-14	2.52-14	2.00-14	2.34-14	6.86-14	1.05
$^{58}Ni(n,p)$:	z = 122.2mm†	2.89-13	0.76-13	0.87-13	1.17-13	2.80-13	0.97
	z = 62.0	3.15-13	0.84-13	0.97-13	1.33-13	3.14-13	1.00
	z = -1.5	3.24-13	0.84-13	0.98-13	1.41-13	3.25-13	1.00
	z = -65.0	3.09-13	0.83-13	0.94-13	1.39-13	3.16-13	1.02
	z = -125.3†	2.73-14	0.73-14	0.83-14	1.24-14	2.80-13	1.03
$^{46}Ti(n,p)$:	z = 122.2mm†	2.37-14	0.65-14	0.71-14	0.92-14	2.28-14	0.96
	z = 62.0	2.80-14	0.73-14	0.79-14	1.04-14	2.56-14	0.91
	z = -1.5	2.81-14	0.75-14	0.80-14	1.09-14	2.64-14	0.94
	z = -65.0	2.71-14	0.72-14	0.76-14	1.08-14	2.56-14	0.94
	z = -125.3†	2.38-14	0.64-14	0.67-14	0.96-14	2.27-14	0.95

*See Table 6.
†See Table 6.
‡See Table 6.

Table 11. Contributions of the Cycle Groups to Additional Calculated SSC-2 Activities at the End of Irradiation and Comparison with HEDL Measurements

	(x,y,z)mm*	E_{EOI}	157C-157E	158C+158D	158E-158G	C_{EOI}	C/E
$^{54}Fe(n,p)$:	(+50,133,-0.6)	7.56-14†	2.69-14	2.14-14	2.41-14	7.24-14	0.96
	(-50,133,-0.6)	7.83-14	2.75-14	2.23-14	2.49-14	7.47-14	0.96
	(25.3,135,-12.7)‡	7.28-14	2.24-14	1.95-14	2.20=14	6.39-14	0.88
	(-25.3,135,-12.7)‡	7.52-14	2.48-14	2.00-14	2.23-14	6.71-14	0.89
$^{46}Ti(n,p)$:	(+39,133,-8.5)**	2.73-14	0.68-14	0.72-14	0.99-14	2.39-14	0.88
	(-39,133,-8.5)**	2.80-14	0.70-14	0.75-14	1.02-14	2.47-14	0.88
$^{58}Ni(n,p)$:	(+43,133,-0.6)**	3.09-13	0.78-13	0.88-13	1.28-13	2.94-13	0.95
	(-43,133,-0.6)**	3.20-13	0.80-13	0.92-13	1.32-132	3.04-13	0.95
$^{63}Cu(n,\alpha)$:	(+43.5,133,-0.6)**	8.91-17	3.30-17	2.41-17	2.56-17	8.27-17	0.93
	(-43.5,133,-0.6)	9.17-17	3.38-17	2.51-17	2.63-17	8.52-17	0.93

*See Table 6.
†See Table 6.
‡Calculations were performed for the locations (±25.3,139,-12.7). No corrections to the measured locations were made.
††Calculations were performed for the locations (±50,133,-0.6). No corrections to the measured locations were made.

Table 12. Contributions of the Cycle Groups to the Calculated SSC-2 Fission Product Activities at the End of Irradiation and Comparison with HEDL Measurements

	(x,y,z)mm*	E_{EOI}†	157C-157E	158C+158D	158E-158G	C_{EOI}	C/E
$^{238}U(n,f)^{137}Cs$:	(+45,133,-8.5)‡	1.07-15**	3.08-16	2.22-16	2.33-16	7.63-16	0.71
	(-45,133,-8.5)	1.15-15	3.15-16	2.32-16	2.39-16	7.86-16	0.68
$^{238}U(n,f)^{95}Zr$:	(+45,133,-8.5)	8.71-14	1.56-14	1.96-14	2.76-14	6.28-14	0.72
	(-45,133,-8.5)	9.38-14	1.59-14	2.04-14	2.83-14	6.46-14	0.69
$^{238}U(n,f)^{103}Ru$:	(+45,133,-8.5)	1.41-13	1.71-14	2.54-14	5.17-14	9.42-14	0.67
	(-45,133,-8.5)	1.55-13	1.74-13	2.66-14	5.31-14	9.71-14	0.63
$^{237}Np(n,f)^{137}Cs$:	(+40.5,133,-8.5)	6.71-15	2.46-15	1.76-15	1.85-15	6.07-15	0.90
	(-40.5,133,-8.5)	6.91-15	2.50-15	1.84-15	1.91-15	6.25-15	0.91
$^{237}Np(n,f)^{95}Zr$:	(+40.5,133,-8.5)	5.87-13	1.36-13	1.60-13	2.38-13	5.34-13	0.91
	(-40.5,133,-8.5)	5.96-13	1.38-13	1.67-13	2.45-13	5.50-13	0.92
$^{237}Np(n,f)^{103}Ru$	(+40.5,133,-8.5)	7.20-13	1.14-13	1.84-13	3.44-13	6.42-13	0.89
	(-40.5,133,-8.5)	7.29-13	1.16-13	1.92-13	3.54-13	6.62-13	0.91

*See Table 6.
†The $^{238}U(n,f)X$ measurements have not been corrected for possible effects of ^{239}Pu burn-in, which may be significant. (See text).
‡All calculations were performed for the locations (±50,133.0,-0.6). No corrections to the measured locations were made.
**See Table 6.

With the exception of the $^{238}U(n,f)X$ activities, which will be discussed later, the agreement between calculations and measurements averages about 10% better for the SSC-2 than for either the SSC-1 or startup comparisons. This better agreement (within about 5%) is caused by average increases in the calculations of about 15% and average increases in the measurements of about 5% over the corresponding SSC-1 values. As will be discussed again later, it begins to appear that the more cycles that are introduced into the calculation, the better the agreement. So far the analysis has proceeded from one cycle (startup) to four cycles (SSC-1) to eight cycles (SSC-2) with improvement in the comparisons with measurement each time. This suggests either that the calculated VENTURE source for a given cycle requires a bias factor which tends to be uncorrelated with that of other cycles, or that some important geometric dimension is changing with the insertion and retraction of the experiment during each cycle but its average value tends to agree with the value assumed in the calculation.

Using the same analytical procedure as outlined for the analyses of the SSC-1 and SSC-2 exposures, but now extended over the full two-year time span, the following results for the calculations in the SPVC were obtained and are shown in Tables 13-19, where comparisons with HEDL measurements (6) also appear.

From an inspection of Tables 14-17, it is evident that the calculations and the measurements agree at "0T", lie within about 5% at T/4, and within about 10% at T/2, with the $^{46}Ti(n,p)$ as usual about 5% more discrepant than either the $^{58}Ni(n,p)$, $^{63}Cu(n,\alpha)$, or the $^{54}Fe(n,p)$ comparisons. (Apparently, the $^{46}Ti(n,p)$ cross sections used in the calculations are about 5% too low.) This agreement is about 5% better at both the T/4 and T/2 locations than in the startup comparisons. Since the two-year measurements average from 10 to 25% lower than the startup in the SPVC on a saturated activity basis, we have shown that this effect is reasonably calculable and is again due to a cycle-to-cycle source variation, especially near the end of the irradiation. The $^{63}Cu(n,\alpha)$ activities reflect truer integrals over the entire irradiation period than any of the other three activities do, again from Tables 14-17, although there seems to be a slight inconsistency at T/4 in the $^{63}Cu(n,\alpha)$ counting rate. The measured $^{54}Fe(n,p)$ saturated activities averaged about 13% lower in the two common SPVC locations (T/4 and T/2) for the two-year exposure than for the startup experiment. A glance at Table 4 verifies that the saturated activities over the course of the two-year exposure average about 10% lower than for the startup experiment. For the $^{58}Ni(n,p)$ and $^{46}Ti(n,p)$ measured saturated activities, the two-year exposure values in the SPVC average about 25% lower. From Tables 15 and 16, better than 90% of these calculated activities at the end of the two-year irradiation come from cycles 158H-158K and later. From Table 4, the saturated activities averaged over these last six cycle groups are about 20% lower than for the startup experiment. This effect of decay can be even more pronounced for some of the fission product activities as is evidenced in Tables 13, 18, and 19. Comparisons of the measured and calculated fission induced activities at the end of irradiation in the

Table 13. Decay Factors to the End of the SPVC + SVBC Irradiation for the Various Cycle Groups

Cycle Group	$^{63}Cu(n,\alpha)$	$^{46}Ti(n,p)$	$^{54}Fe(n,p)$	$^{58}Ni(n,p)$	$(n,f)^{137}Cs$	$(n,f)^{95}Zr$	$(n,f)^{103}Ru$	$(n,f)^{140}Ba$
153B+153C	0.005606	2.847-4	0.008196	1.043-4	0.001230	5.202-5	4.538-7	7.425-19
153D	0.004268	2.530-4	0.006480	9.55-5	9.325-4	4.855-5	4.822-7	1.574-18
153F	0.003081	2.118-4	0.004844	8.22-5	6.694-4	4.261-5	4.800-7	3.073-18
153G-154C	0.01368	0.001237	0.02295	5.085-4	0.002942	2.736-4	3.956-6	1.120-16
154D-154J	0.02269	0.003592	0.04325	0.001648	0.004769	9.558-4	2.281-5	1.171-14
155B-155F	0.01262	0.003899	0.02821	0.002027	0.002587	0.001280	5.281-5	4.228-13
155G-156B	0.01772	0.008289	0.06198	0.004669	0.003577	0.003115	1.850-4	1.160-11
156C-157B	0.02122	0.1696	0.05926	0.01059	0.004205	0.007575	7.150-4	5.858-10
157C-157E	0.01328	0.01657	0.04116	0.01125	0.002582	0.008521	0.001161	5.943-9
158C+158D	0.009193	0.1664	0.3110	0.1213	0.001762	0.009635	0.001795	4.728-8
158E-158G	0.01121	0.02637	0.04031	0.02020	0.002127	0.01661	0.003881	3.553-7
158H-158K	0.01666	0.05543	0.06495	0.04541	0.003122	0.03909	0.01237	6.333-6
159A-159C	0.01957	0.1016	0.08465	0.04541	0.003122	0.03909	0.01237	6.333-6
159D-160C	0.02159	0.1920	0.1059	0.1899	0.003898	0.1859	0.1374	0.007425
160D-160E	0.007316	0.09073	0.03886	0.09546	0.001304	0.09742	0.09392	0.01761
161B	0.008680	0.1428	0.04925	0.1586	0.001530	0.1680	0.2064	0.1455
161C	0.009366	0.1939	0.05609	0.2251	0.001638	0.2456	0.3676	0.7565

Table 14. Contributions of the Cycle Groups to the Calculated SPVC and SVBC Activities at the End of Irradiation and Comparison with HEDL Measurements for $^{54}Fe(n,p)$

Cycle Group	"OT"*	T/4*	T/2*	VEPCO*
153B+153C	3.65-16†	1.53-16	5.59-17	3.07-18
153D	3.21-16	1.35-16	4.92-17	2.70-18
153F	2.32-16	9.73-17	3.55-17	1.93-18
153G-154C	1.53-16	3.57-16	1.30-16	7.09-18
154D-154J	1.81-15	7.58-16	2.77-16	1.54-17
155B-155F	1.44-15	6.02-16	2.20-16	1.22-17
155G-156B	2.81-15‡	1.18-15‡	4.29-16‡	2.38-17‡
156C-157B	2.87-15	1.20-15	4.40-16	2.42-17
157C-157E	2.04-15	8.53-16	3.12-16	1.71-17
158C+158D	1.65-15	6.91-16	2.52-16	1.43-17
158E-158G	1.83-15	7.64-16	2.79-16	1.42-17
158H-158K	3.29-15	1.38-15	5.02-16	1.43-17
159A-159C	3.75-15	1.57-15	5.71-16	3.03-17
159D-160C	4.75-15	1.98-15	7.22-16	3.89-17
160D+160E	1.78-15	7.45-16	2.72-16	1.48-17
161B	2.32-15	9.72-16	3.54-16	1.89-17
161C	2.53-15	1.06-15	3.87-16	2.10-17
SUM, CALC.	3.46-14	1.45-14	5.29-15	2.88-16
MEASURED	3.40-14	1.51-14	5.87-15	--
C/E	1.02	0.96	0.90	

*The SPVC locations "OT", T/4 and T/2 have coordinates (x,y,z) of (± 53.7, 241.3, -8.5) mm, (± 53.7, 286.4, -8.5) mm, and (± 53.7, 337.8, -8.5), respectively, based on the HEDL coordinate system, and the SVBC location in the VEPCO capsule has coordinates (-72.6, 765.0, 55.3) mm. Both the measured and calculated activities vary little between the + 53.7 and -53.7 locations, so that only the average of the activities at the two x locations appears in this table.

†Read 3.65×10^{-16} disintegrations per second per atom, etc.

‡Estimated

Table 15. Contributions of the Cycle Groups to the Calculated SPVC and SVBC Activities at the End of Irradiation and Comparison with HEDL Measurements for $^{46}Ti(n,p)$

Cycle Group	"OT"*	T/4*	T/2*	VEPCO*
153B+153C	1.73-18†	7.08-19	2.55-19	1.56-20
153D	1.72-18	7.03-19	2.52-19	1.55-20
153F	1.39-18	5.70-19	2.04-19	1.24-20
153G-154C	6.30-18	2.57-18	9.23-19	5.60-20
154D-154J	2.06-17	8.43-18	3.02-18	1.88-19
155B-155F	2.72-17	1.11-17	3.97-18	2.47-19
155G-156B	5.14-17‡	2.10-17‡	7.51-18‡	4.66-19‡
156C-157B	1.13-16	4.60-17	1.65-17	1.01-18
157C-157E	1.12-16	4.58-17	1.64-17	1.01-18
158C+158D	1.21-16	4.92-17	1.77-17	1.12-18
158E-158G	1.64-16	6.68-17	2.38-17	1.43-18
158H-158K	3.86-16	1.58-16	5.64-17	3.40-18
159A-159C	6.18-16	2.53-16	8.96-17	5.33-18
159D-160C	1.18-15	4.82-16	1.73-16	1.03-17
160D+160E	5.75-16	2.34-16	8.40-17	5.09-18
161B	9.32-16	3.81-16	1.37-16	8.07-18
161C	1.22-15	4.95-16	1.78-16	1.07-17
SUM, CALC.	5.53-15	2.26-15	8.10-16	4.85-17
MEASURED	5.90-15	2.57-15	9.45-16	--
C/E	0.94	0.88	0.86	

*See Table 14.
†See Table 14.
‡See Table 14.

Table 16. Contributions of the Cycle Groups to the Calculated SPVC and SVBC Activities at the End of Irradiation and Comparison with HEDL Measurements for $^{58}Ni(n,p)$

Cycle Group	"OT"*	T/4*	T/2*	VEPCO*
153B+153C	6.29-18†	2.69-18	1.01-18	5.52-20
153D	6.40-18	2.75-18	1.02-18	5.62-20
153F	5.34-18	2.28-18	8.55-19	4.63-20
153G-154C	2.68-17	1.15-17	4.28-18	2.32-19
154D-154J	9.71-17	4.17-17	1.56-17	8.62-19
155B-155F	1.45-16	6.19-17	2.31-17	1.28-18
155G-156B	2.95-16‡	1.27-16‡	4.74-17‡	2.60-18‡
156C-157B	7.12-16	3.05-16	1.14-16	6.26-18
157C-157E	7.54-16	3.23-16	1.21-16	6.60-18
158C+158D	8.68-16	3.73-16	1.40-16	7.86-18
158E-158G	1.24-15	5.31-16	1.98-16	1.07-17
158H-158K	3.12-15	1.34-15	4.97-16	2.68-17
159A-159C	5.44-15	2.33-15	8.67-16	4.59-17
159D-160C	1.15-14	4.93-15	1.83-15	9.82-17
160D+160E	5.92-15	2.54-15	9.48-16	5.13-17
161B	1.00-14	4.33-15	1.62-15	8.57-17
161C	1.38-14	5.87-15	2.21-15	1.19-16
SUM, CALC.	5.39-14	2.31-14	8.64-15	4.64-16
MEASURED	5.44-14	2.45-14	9.61-15	--
C/E	0.99	0.94	0.90	

*See Table 14.
†See Table 14.
‡See Table 14.

Table 17. Contributions of the Cycle Groups to the Calculated SPVC and SVBC Activities at the End of Irradiation and Comparison with HEDL Measurements for $^{63}Cu(n,\alpha)$

Cycle Group	"OT"*	T/4*	T/2*	VEPCO*
153B+153C	1.91-18†	8.00-19	2.95-19	1.96-20
153D	1.62-18	6.78-19	2.51-19	1.66-20
153F	1.13-18	4.73-19	1.75-19	1.15-20
153G-154C	3.90-18	1.63-18	6.01-19	3.94-20
154D-154J	7.26-18	3.04-18	1.13-18	7.55-20
155B-155F	4.90-18	2.05-18	7.57-19	5.07-20
155G-156B	6.13-18‡	2.57-18‡	9.47-19‡	6.33-20‡
156C-157B	7.88-18	3.31-18	1.22-18	8.09-20
157C-157E	5.02-18	2.10-18	7.75-19	5.12-20
158C+158D	3.71-18	1.55-18	5.75-19	3.93-20
158E-158G	3.88-18	1.62-18	5.98-19	3.87-20
158H-158K	6.49-18	2.72-18	9.99-19	6.50-20
159A-159C	6.66-18	2.79-18	1.02-18	6.52-20
159D-160C	7.43-18	3.10-18	1.14-18	7.38-20
160D+160E	2.59-18	1.09-18	4.01-19	2.63-20
161B	3.17-18	1.33-18	4.90-19	3.13-20
161C	3.29-18	1.38-18	5.09-19	3.32-20
SUM, CALC.	7.70-17	3.70-17	1.19-17	7.82-19
MEASURED	8.24-17	3.64-17	1.39-17	--
C/E	0.93	1.02	0.86	

*See Table 14.
†See Table 14.
‡See Table 14.

Table 18. Contributions of the Cycle Groups to the Calculated SPVC Fission Product Activities at the End of Irradiation for $^{238}U(n,f)X$ and Comparison with HEDL Measurements

Cycle Group	"OT"*				T/4*				T/2*			
	^{137}Cs	^{95}Zr	^{103}Ru	^{140}Ba	^{137}Cs	^{95}Zr	^{103}Ru	^{140}Ba	^{137}Cs	^{95}Zr	^{103}Ru	^{140}Ba
153B+153C	1.67-17†	6.02-19	6.40-21	1.00-32	8.08-18	2.91-19	3.10-21	4.84-33	3.37-18	1.21-19	1.29-21	2.01-33
153D	1.41-17	6.26-19	7.58-21	2.36-32	6.80-18	3.02-19	3.66-21	1.14-32	2.84-18	1.26-19	1.53-21	4.78-33
153F	9.80-18	5.31-19	7.30-21	4.46-32	4.74-18	2.57-19	3.53-21	2.16-32	1.97-18	1.07-19	1.47-21	8.97-33
153G-154C	3.34-17	2.64-18	4.66-20	1.26-30	1.61-17	1.27-18	2.25-20	6.07-31	6.72-18	5.31-19	9.38-21	2.54-31
154D-154J	6.08-17	1.04-17	3.02-19	1.48-28	2.92-17	4.99-18	1.45-19	7.11-29	1.22-17	2.09-18	6.06-20	2.97-29
155B-155F	4.03-17	1.70-17	8.54-19	6.53-27	1.94-17	8.18-18	4.11-19	3.14-27	8.08-18	3.41-18	1.71-19	1.31-27
155G-156B*	4.96-17	3.67-17	2.66-18	1.59-25	2.39-17	1.77-17	1.28-18	7.66-26	9.95-18	7.38-18	5.34-19	3.20-26
156C-157B	6.24-17	9.56-17	1.10-17	8.60-24	3.00-17	4.60-17	5.29-18	4.13-24	1.25-17	1.92-17	2.20-18	1.72-24
157C-157E	3.91-17	1.10-16	1.83-17	8.93-23	1.88-17	5.29-17	8.80-18	4.29-23	7.84-18	2.21-17	3.67-18	1.79-23
158C+158D	2.85-17	1.33-16	3.02-17	7.59-22	1.38-17	6.44-17	1.46-17	3.68-22	5.74-18	2.68-17	6.08-18	1.53-22
158E-158G	2.95-17	1.96-16	5.59-17	4.89-21	1.42-17	9.43-17	2.69-17	2.35-21	5.91-18	3.93-17	1.12-17	9.80-22
158H-158K	4.82-17	5.13-16	1.98-16	9.69-20	2.31-17	2.46-16	9.49-17	4.64-20	9.63-18	1.02-16	3.96-17	1.94-20
159A-159C	4.86-17	9.48-16	5.38-16	2.21-18	2.33-17	4.54-16	2.58-16	1.06-18	9.72-18	1.90-16	1.08-16	4.42-19
159D-160C	5.29-17	2.15-15	1.94-15	9.99-17	2.54-17	1.03-15	9.31-16	4.80-17	1.06-17	4.31-16	3.89-16	2.00-17
160D-160E	1.81-17	1.15-15	1.35-15	2.43-16	8.68-18	5.51-16	6.47-16	1.17-16	3.62-18	2.30-16	2.70-16	4.86-17
161B	2.19-17	2.05-15	3.07-15	2.06-15	1.06-17	9.92-16	1.49-15	9.97-16	4.36-18	4.08-16	6.11-16	4.10-16
161C	2.23-17	2.85-15	5.20-15	1.02-14	1.08-17	1.38-15	2.52-15	4.94-15	4.47-18	5.71-16	1.04-15	2.04-15
SUM,CALC.	5.96-16	1.03-14	1.24-14	1.27-14	2.87-16	4.94-15	6.00-15	6.11-15	1.20-16	2.05-15	2.48-15	2.52-15
MEASURED**	9.17-16	1.67-14	2.31-14	--	3.56-16	5.74-15	7.71-15	--	1.43-16	2.32-15	2.96-15	--
C/E	0.65	0.62	0.54		0.81	0.86	0.78		0.84	0.88	0.84	

*See Table 14.
†See Table 14.
*See Table 14.
**Not corrected for effects of ^{239}Pu burn-in, which may be significant at OT and T/4. (See Text).

Table 19. Contributions of the Cycle Groups to the Calculated SPVC Fission Product Activities at the End of Irradiation for $^{237}Np(n,f)X$ and Comparison with HEDL Measurements

	"0T"*				T/4*				T/2*			
Cycle Group	^{137}Cs	^{95}Zr	^{103}Ru	^{140}Ba	^{137}Cs	^{95}Zr	^{103}Ru	^{140}Ba	^{137}Cs	^{95}Zr	^{103}Ru	^{140}Ba
153B+153C	1.26-16†	4.83-18	4.13-20	6.64-32	7.78-17	2.98-18	2.55-20	4.10-32	4.26-17	1.63-18	1.40-20	2.25-32
153D	1.07-16	5.02-18	4.89-20	1.57-31	6.58-17	3.09-18	3.01-20	9.66-32	3.60-17	1.70-18	1.66-20	5.35-32
153F	7.37-17	4.26-18	4.71-20	2.96-31	4.55-17	2.63-18	2.90-20	1.83-31	2.49-17	1.44-18	1.60-20	1.00-31
153G-154C	2.51-16	2.12-17	3.01-19	8.37-30	1.55-16	1.30-17	1.85-19	2.49-17	1.44-18	1.60-20	1.02-19	2.84-30
154D-154J	4.58-16	8.34-17	1.95-18	9.83-28	2.83-16	5.11-17	1.19-18	6.02-18	1.55-16	2.82-17	6.58-19	3.32-28
155B-155F	3.03-16	1.36-16	5.51-18	4.34-26	1.88-16	8.38-17	3.38-18	2.66-26	1.02-16	4.59-17	1.86-18	1.47-26
155G-156B*	3.73-16	2.94-16	1.72-17	1.06-24	2.31-16	1.81-16	1.05-17	6.49-25	1.26-16	9.94-17	5.80-18	3.58-25
156C-157B	4.69-16	7.67-16	7.10-17	5.71-23	2.90-16	4.71-16	7.35-17	3.50-23	1.59-16	2.59-17	2.39-17	1.93-23
157C-157E	2.93-16	8.83-16	1.18-16	5.93-22	1.81-16	5.42-16	7.24-17	3.63-22	9.92-17	2.98-16	3.98-17	2.00-22
158C+158D	2.14-16	1.07-15	1.95-16	5.04-21	1.33-16	6.59-16	1.20-16	3.12-21	7.28-17	3.61-16	6.60-17	1.71-21
158E-158G	2.20-16	1.57-15	3.71-16	3.25-20	1.36-16	9.66-16	2.21-16	1.99-20	7.45-17	5.29-16	1.22-16	1.10-20
158H-158K	3.59-16	4.12-15	1.28-15	6.43-19	2.22-16	2.52-15	7.81-16	3.93-19	1.21-16	1.37-15	4.30-16	2.17-19
159A-159C	3.62-16	7.61-15	3.47-15	1.47-17	2.23-16	4.65-15	2.12-15	8.98-18	1.22-16	2.56-15	1.17-15	1.95-18
159D-160C	3.94-16	1.73-14	1.25-14	6.63-16	2.44-16	1.05-14	7.66-15	4.07-16	1.33-16	5.81-15	4.22-15	2.24-16
160D-160E	1.35-16	9.23-15	8.71-15	1.61-15	8.31-17	5.64-15	5.32-15	9.91-16	4.54-17	3.10-15	2.93-15	5.44-16
161B	1.62-16	1.64-14	1.98-14	1.37-14	1.01-16	1.02-14	1.23-14	8.45-15	5.46-17	5.50-15	6.63-15	4.59-15
161C	1.65-16	2.25-14	3.30-14	6.69-14	1.02-16	1.39-14	2.04-14	4.14-14	5.59-17	7.62-15	1.12-14	2.26-14
SUM,CALC.	4.47-15	8.20-14	7.96-14	8.29-14	2.76-15	5.03-14	4.90-14	5.13-14	1.51-15	2.76-14	2.67-14	2.79-14
MEASURED	5.10-15	8.62-14	8.54-14	--	3.06-15	5.13-14	5.09-14	--	1.69-15	2.84-14	2.84-14	--
C/E	0.88	0.95	0.93		0.90	0.98	0.96		0.89	0.97	0.94	

*See Table 14.
†See Table 14.
*See Table 14.

SPVC in Tables 18 and 19 show that the $^{238}U(n,f)X$ activities are severely undercalculated at OT and slightly undercalculated at T/4, whereas the calculated and measured $^{237}Np(n,f)X$ activities agree to around 5-10% at all three locations.

Since the contributions from $^{235}U(n,f)X$ contamination were considered and subtracted in the HEDL data reduction (6), and effects from photofission are estimated to be small, the remaining possibility of ^{239}Pu burn-in arising from the $^{238}U(n,\gamma)$ reaction with a consequent $^{239}Pu(n,f)X$ contribution to the measurements requires evaluation. Subsequent calculations by both HEDL (7) and ORNL (8) now indicate non-negligible contributions from ^{239}Pu burn-in should occur in regions of relatively high fluence, affecting for example the measurements in the SSC-2 and at the OT location in the SPVC in particular. Thus, consideration of ^{239}Pu burn-in can explain the relatively poor agreement between calculation and measurement of the $^{238}U(n,f)X$ activities at some locations. The combined effects of ^{235}U contamination, photofission sensitivity, and ^{239}Pu burn-in may well compromise the usefulness of the $^{238}U(n,f)X$ reaction as a dosimeter for some applications.

Conclusions

An important conclusion derived from this study is that cycle-to-cycle variations in the ORR core leakages are as much as 40%, and account for most of the difference in fluence rate levels observed between the startup and two-year experiments. Secondly, the C/E comparisons indicate better general agreement in the present experiment than either the PCA or the startup experiments, and the resulting calculated spectral fluences available for metallurgical analysis and/or adjustment described in the appendix should be accurate to within about 10%. Finally, evidence for the seeming importance of ^{239}Pu burn-in as yet another necessary correction to $^{238}U(n,f)X$ dosimeter measurements in regions of relatively high fluence has been presented, perhaps further compromising the usefulness of this dosimeter.

References

1. Ketema, D. J., H. J. Nolthenius and W. L. Zijp, Neutron Metrology in the ORR: ECN Activity and Fluence Measurements for the LW Pressure Vessel Surveillance Dosimetry Program, ECN-80-164, Petten, the Netherlands (1980).

2. Ketema, D. J., H. J. Nolthenius and W. L. Zijp, Neutron Metrology in the ORR: Second Contribution of ECN Activity and Fluence Measurements for the LWR Pressure Vessel Surveillance Dosimetry Program, ECN-81-097, Petten, the Netherlands (1981).

3. Lippincott, E. P. and L. S. Kellogg, HEDL, Informal Communication to Distribution. Preliminary Measured Results (1982).

References (cont'd)

4. Maerker, R. E., M. L. Williams, B. L. Broadhead, J. J. Wagschal and C. Y. Fu, Revision and Expansion of the Database in the LEPRICON Dosimetry Methodology, EPRI Report (to be published in 1984).

5. Lillie, R. A., private communication. About half of the cycles active during the two-year irradiation (153G-155G, 156C-158F) had previously been calculated with VENTURE, but without FISSOR files. These runs by Lillie were restarted and converged with FISSOR files written. The remaining cycles were calculated for the first time using VENTURE by B. A. Worley and R. A. Lillie, with both FLUX and FISSOR files written. The authors are greatly indebted to Dr. Lillie for providing access to the earlier runs as well as assisting in running some of the later ones.

6. Lippincott, E. P. and L. S. Kellogg, HEDL, Informal Communication to Distribution. Updated Measured Results (1984).

7. Lippincott, E. P. and R. L. Simons, HEDL, Informal Communication to Distribution (1984).

8. Stallmann, F. W., Determination of Damage Exposure Values in the PSF Metallurgical Irradiation Experiment, NUREG/CR-3814, ORNL/TM-9166 (1984).

APPENDIX

Description of the Contents of the Spectral Fluence Tape X13850*

All 50 files are BCD and use a fixed 6E12.5 format. The tape is non-labeled and has the following general JCL:

```
//GØ.FTXXF001 DD UNIT=TAPE8,LABEL=(YY,NL,,IN),DISP=(ØLD,KEEP),
//   DCB=(RECFM=FB,LRECL=72,BLKSIZE=7200,DEN=3),VØL=SER=X13850
```

where

XX is the logical tape number for a given file YY to be read, and

XX can be any number between 01 and 99 except 05, 06, 07, and 53, and

YY can be any number between 1 and 50.

File 1 contains the upper energy limits of each of the 38 energy groups in eV, and a 39th entry is the lower energy limit of the 38th group. (39 entries)

File 2 contains the midpoint values of the axial mesh that describes all the vertical profiles in files 3-50. These z values may be assumed to be the point axial locations at which the fluences in files 3-50 are accumulated. These coordinates follow the HEDL scheme, i.e., they are relative to a horizontal plane 5.08 cm below the midplane, and are negative below this plane and positive above. These 21 values are expressed in cm, and represent the spatial order in which the fluences appear. These 21 values cover the entire axial range of the locations of all the metallurgical specimens used in the 2-year exposure, and are, in order:

```
27.94,  23.02,  20.165,  18.735,  17.465,  16.195,  13.97,
11.43,   9.69,   8.42,    6.20,    3.66,    1.27,   -0.85,
-3.665, -6.625, -8.56,  -10.0,   -11.6,   -13.97   -16.195
```

Files 3-50 each contain spectral fluence profiles, each file representing the spectral fluence profiles for a given x and y location and irradiation history. Thus, files 3-10 contain the spectral fluence axial profiles for the SSC-2 irradiation exposure, files 11-42 the profiles for the SPVC and SVBC full 2-year exposure, and files 43-50 the profiles for the SSC-1 irradiation exposure. Both the SSC-1 and SSC-2 files consider the same eight (x,y) locations, file 3 corresponding to the same (x,y) location as file 43, file 4 the same as file 44, and so on up to file 10 and file 50. The SPVC and SVBC 2-year exposures appearing in files 11-42 are at thirty-two (x,y) locations, one (x,y) location for each file. The following table summarizes the contents of each file.

*Copies of this tape may be obtained by contacting F.B.K. Kam, Oak Ridge National Laboratory, P.O. Box X, Oak Ridge, TN 37831.

Table A1. Contents of the Spectral Fluence Axial Profile Tape

File No.	Description*
1	Energy grid of the first 38 ELXSIR groups in eV (39 entries)
2	Axial locations at which the profiles are given, in cm. (21)
3	Accumulated fluences in neutrons/cm^2 as a function of energy and axial location for the SSC-2 exposure. (x,y)=(-10.37,12.221)cm. (798)
4	Same as for file 3 except (x,y)=(10.37,12.221)
5	Same as for file 3 except (x,y)=(0.0,12.655)
6	Same as for file 3 except (x,y)=(-4.572,13.290)
7	Same as for file 3 except (x,y)=(4.572,13.290)
8	Same as for file 3 except (x,y)=(0.0,13.925)
9	Same as for file 3 except (x,y)=(-10.37,14.359)
10	Same as for file 3 except (x,y)=(10.37,14.359)
11	Accumulated fluences in neutrons/cm^2 as a function of energy and axial location for the full two-year exposure. This is a special point 1/4 inch inside the aluminum window: (x,y)=(0.0,-0.685)cm.
12	Same as for file 11 except (x,y)=(0.0,19.606), another special point 2.264 cm in front of the SPVC
13	Same as for file 11 except (x,y)=(-10.37,22.981) "0T" location
14	Same as for file 11 except (x,y)=(10.37,22.981) "0T" location
15	Same as for file 11 except (x,y)=(0.0,23,415) "0T" location
16	Same as for file 11 except (x,y)=(-4.572,24.050) "0T" location
17	Same as for file 11 except (x,y)=(4.572,24.050) "0T" location
18	Same as for file 11 except (x,y)=(0.0,24.685) "0T" location
19	Same as for file 11 except (x,y)=(-10.37,25.119) "0T" location
20	Same as for file 11 except (x,y)=(10.37,25.119) "0T" location
21	Same as for file 11 except (x,y)=(-10.37,27.491) T/4 location
22	Same as for file 11 except (x,y)=(10.37,27.491) T/4 location
23	Same as for file 11 except (x,y)=(0.0,27.925) T/4 location
24	Same as for file 11 except (x,y)=(-4.572,28.560) T/4 location
25	Same as for file 11 except (x,y)=(4.572,28.560) T/4 location
26	Same as for file 11 except (x,y)=(0.0,29.195) T/4 location
27	Same as for file 11 except (x,y)=(-10.37,29.629) T/4 location
28	Same as for file 11 except (x,y)=(10.37,29.629) T/4 location
29	Same as for file 11 except (x,y)=(-10.37,32.631) T/2 location
30	Same as for file 11 except (x,y)=(10.37,32.631) T/2 location
31	Same as for file 11 except (x,y)=(0.0,33.065) T/2 location
32	Same as for file 11 except (x,y)=(-4.572,33.70) T/2 location
33	Same as for file 11 except (x,y)=(4.572,33.70) T/2 location
34	Same as for file 11 except (x,y)=(0.0,34.335) T/2 location
35	Same as for file 11 except (x,y)=(-10.37,34.769) T/2 location
36	Same as for file 11 except (x,y)=(10.37,34.769) T/2 location
37	Same as for file 11 except (x,y)=(0.0,38.455), a special point 5.945 cm inside the SPVC as measured from the back face; a nominal 3T/4 location

Table A1. (cont'd)

File No.	Description*
38	Same as for file 11 except (x,y)=(0.0,43.925), another special point 0.475 cm inside the SPVC as measured from the back face; a nominal full T location
39	Same as for file 11 except (x,y)=(-10.37,76.709) SVBC(VEPCO) location
40	Same as for file 11 except (x,y)=(-4.872,76.709) SVBC(VEPCO) location
41	Same as for file 11 except (x,y)=(4.872,76.709) SVBC(VEPCO) location
42	Same as for file 11 except (x,y)=(10.37,76.709) SVBC(VEPCO) location
43	Accumulated fluences in neutrons/cm^2 as a function of energy and axial location for the SSC-1 exposure. (x,y)=(-10.37,12.221)cm
44	Same as for file 43 except (x,y)=(10.37,12.221)
45	Same as for file 43 except (x,y)=(0.0,12.655)
46	Same as for file 43 except (x,y)=(-4.572,13.290)
47	Same as for file 43 except (x,y)=(4.572,13.290)
48	Same as for file 43 except (x,y)=(0.0,13.925)
49	Same as for file 43 except (x,y)=(-10.37,14.359)
50	Same as for file 43 except (x,y)=(10.37,14.359)

*The origin for the x-axis is the same as the HEDL scheme with negative values to the south. The origin for the y-axis also follows the HEDL scheme, but the y-dimensions are based not on the nominal values used by HEDL but actually measured water gap thicknesses, as used by C. A. Baldwin in his description of the absolute notch locations of the metallurgical specimens. The transport calculations assumed the thermal shield to be 6.00 cm. thick instead of 5.99 used by Baldwin and the thickness of the biggest water gap to be 6.17 cm. rather than the 6.13 used by Baldwin. All locations within the SSC, SPVC, and SVBC have been adjusted in the calculations to reflect these slight differences, and no further adjustment of the calculated values to either the HEDL locations for dosimetry or the Baldwin locations for metallurgy are necessary.

The fluences are read from file YY by such statements as

```
      DØ 1 K=1,21
    1 READ(XX,2)(FLUENS(IG,K),IG=1,38)
    2 FØRMAT(6E12.5)
      REWIND XX
```

where XX is the logical tape number assigned to file YY. Thus the fluence spectrum at each axial location constitutes a logical record. The fluences above 1 MeV (grps. 1-27) for each of the 21 axial locations in files 6, 16, 24, 32, 40, and 46 appear in Table A2. From axial comparisons previously shown in Tables 6 and 10, the fluence rate synthesis procedure expressed by Eq. (4) may be beginning to underestimate the fluences in the neighborhood of z=12.2cm and above, and perhaps overestimate the fluences in the neighborhood of z=-12.5cm and below.

Table A2. Fluence Above 1MeV Axial Profiles Near x =-4.572 for Typical SSC-1, "0T," T/4, T/2, SVBC, and SSC-2 Metallurgical Specimen Locations

z*	SSC-1	0T	T/4	T/2	SVBC	SSC-2
27.94	7.02+18†	2.08+19	1.14+19	5.43+18	3.64+17	1.62+19
23.02	9.44+18	2.65+19	1.44+19	6.84+18	4.05+17	2.19+19
20.165	1.37+19	3.01+19	1.63+19	7.82+18	4.14+17	3.21+19
18.735	1.68+19	3.17+19	1.75+19	8.40+18	4.25+17	3.94+19
17.465	1.70+19	3.39+19	1.94+19	9.25+18	4.30+17	3.98+19
16.195	1.68+19	3.33+19	1.83+19	8.71+18	4.40+17	3.94+19
13.97	1.84+19	3.44+19	1.87+19	8.81+18	4.53+17	4.32+19
11.43	1.96+19	3.55+19	1.92+19	8.97+18	4.77+17	4.64+19
9.69	2.02+19	3.61+19	1.94+19	9.08+18	4.98+17	4.79+19
8.42	2.07+19	3.67+19	1.97+19	9.17+18	5.17+17	4.93+19
6.20	2.13+19	3.77+19	2.02+19	9.32+18	5.22+17	5.09+19
3.66	2.17+19	3.83+19	2.04+19	9.42+18	5.18+17	5.20+19
1.27	2.19+19	3.86+19	2.06+19	9.47+18	5.13+17	5.26+19
-0.85	2.18+19	3.86+19	2.05+19	9.44+18	5.07+17	5.25+19
-3.665	2.17+19	3.85+19	2.04+19	9.38+18	5.07+17	5.23+19
-6.625	2.10+19	3.73+19	1.98+19	9.13+18	5.00+17	5.08+19
-8.56	2.04+19	3.63+19	1.93+19	8.91+18	4.93+17	4.93+19
-10.0	1.97+19	3.54+19	1.88+19	8.71+18	4.73+17	4.76+19
-11.6	1.90+19	3.44+19	1.83+19	8.51+18	4.49+17	4.59+19
-13.97	1.76+19	3.26+19	1.75+19	8.19+18	4.26+17	4.26+19
-16.195	1.58+19	3.03+19	1.67+19	7.91+18	4.10+17	3.83+19

*Centimeters above the approximate axial location of peak flux, 5.08 cm below the reactor horizontal midplane.
†Read 7.02×10^{18} neutrons/cm^2, etc.

NUREG/CR-3886
ORNL/TM-9265
Distribution Category R5

INTERNAL DISTRIBUTION

1-2. L. S. Abbott
3. C. A. Baldwin
4. D. G. Cacuci
5. P. W. Dickson, Jr. (Consultant)
6. D. M. Eissenberg
7. G. H. Golub (Consultant)
8. F. B. K. Kam
9-13. R. E. Maerker
14. F. C. Maienschein
15. A. P. Malinauskas
16. F. R. Mynatt
17. F. W. Stallmann
18. D. Steiner (Consultant)
19. C. R. Weisbin
20-24. B. A. Worley
25. A. Zucker
26. Central Research Library
27. ORNL Y-12 Technical Library-Document Reference Section
28. Laboratory Records
29. ORNL Patent Office
30. Laboratory Records - RC

EXTERNAL DISTRIBUTION

31. Office of Assistant Manager for Energy Research and Development, DOE-ORO, Oak Ridge, TN 37831.
32. C. Z. Serpan, Jr., Division of Engineering Technology, U.S. Office of NRC, MS-SS-1130, Washington, DC 20555.
33-34. Technical Information Center (TIC).
35-385. Given distribution as shown in NRC Category R5, Water Reactor Safety Research - Metallurgy and Materials (10 copies - NTIS).

NRC FORM 335 (2 84) NRCM 1102 3201, 3202

U.S. NUCLEAR REGULATORY COMMISSION

BIBLIOGRAPHIC DATA SHEET

SEE INSTRUCTIONS ON THE REVERSE

1. REPORT NUMBER (Assigned by TIDC add Vol. No., if any)

NUREG/CR-3886
ORNL/TM-9265

2. TITLE AND SUBTITLE

ACTIVITY AND FLUENCE CALCULATIONS FOR THE STARTUP AND TWO-YEAR IRRADIATION EXPERIMENTS PERFORMED AT THE POOLSIDE FACILITY

3. LEAVE BLANK

4. DATE REPORT COMPLETED

MONTH	YEAR
August	1984

5. AUTHOR(S)

R. E. Maerker and B. A. Worley

6. DATE REPORT ISSUED

MONTH	YEAR
September	1984

7. PERFORMING ORGANIZATION NAME AND MAILING ADDRESS (Include Zip Code)

Oak Ridge National Laboratory
P.O. Box X
Oak Ridge, Tennessee 37831

8. PROJECT/TASK/WORK UNIT NUMBER

9. FIN OR GRANT NUMBER

B0415

10. SPONSORING ORGANIZATION NAME AND MAILING ADDRESS (Include Zip Code)

Division of Engineering Technology
Office of Nuclear Regulatory Research
U.S. Nuclear Regulatory Commission
Washington, DC 20555

11a. TYPE OF REPORT

Topical

b. PERIOD COVERED (Inclusive dates)

Oct. - Dec. 1983

12. SUPPLEMENTARY NOTES

13. ABSTRACT (200 words or less)

This report is based on two separate intra-laboratory correspondences to F. B. K. Kam of the Operations Division from the authors, dated August 8 and October 21, 1983, detailing results of an analysis of two experiments performed at the Poolside Facility. It expands somewhat on the comparisons between measurement and calculation for the two-year experiment over those that were originally presented in the correspondence because of the recent availability of additional measured results. The two experiments analyzed in this report represent a scoping short-term dosimetry experiment and a long-term experiment using virtually the same geometry but incorporating metallurgical specimens as well as dosimetry. The long-term experiment is intended as an international metallurgical benchmark, and the fluence calculations described in this report have been made available to the international reactor dosimetry community to be used in their damage assessment studies and/or adjustment procedures.

14. DOCUMENT ANALYSIS - a. KEYWORDS/DESCRIPTORS

b. IDENTIFIERS/OPEN-ENDED TERMS

15. AVAILABILITY STATEMENT

Unlimited

16. SECURITY CLASSIFICATION

(This page)
Unclassified

(This report)
Unclassified

17. NUMBER OF PAGES

46

18. PRICE

120555078877 1 1ANIRS
US NRC
ADM-DIV OF TIDC
POLICY & PUB MGT BR-PDR NUREG
W-501
WASHINGTON DC 20555